2-1-2022

Functional dissociation of behavioral effects from acetylcholine and glutamate released from cholinergic striatal interneurons

Ornela Kljakic
Robarts Research Institute

Helena Janíčková
Robarts Research Institute

Miguel Skirzewski
Robarts Research Institute

Amy Reichelt
Robarts Research Institute

Sara Memar
Robarts Research Institute

See next page for additional authors

Received: 12 September 2021 | Revised: 3 December 2021 | Accepted: 17 December 2021

DOI: 10.1096/fj.202101425R

THE FASEB JOURNAL

RESEARCH ARTICLE

Functional dissociation of behavioral effects from acetylcholine and glutamate released from cholinergic striatal interneurons

Ornela Kljakic[1,2] | Helena Janíčková[1] | Miguel Skirzewski[1,3] | Amy Reichelt[1,4] | Sara Memar[1,3] | Salah El Mestikawy[5,6] | Yulong Li[7] | Lisa M. Saksida[1,3,4] | Timothy J. Bussey[1,3,4] | Vania F. Prado[1,2,3,4] | Marco A. M. Prado[1,2,3,4]

[1]Translational Neuroscience Group, Robarts Research Institute, Schulich School of Medicine & Dentistry, The University of Western Ontario, London, Ontario, Canada

[2]Department of Anatomy and Cell Biology, Schulich School of Medicine & Dentistry, The University of Western Ontario, London, Ontario, Canada

[3]Brain and Mind Institute, The University of Western Ontario, London, Ontario, Canada

[4]Department of Physiology and Pharmacology, Schulich School of Medicine & Dentistry, The University of Western Ontario, London, Ontario, Canada

[5]Department of Psychiatry, Douglas Mental Health University Institute, McGill University, Montreal, Quebec, Canada

[6]INSERM, CNRS, Neuroscience Paris Seine – Institut de Biologie Paris Seine (NPS – IBPS), Sorbonne Université, Paris, France

[7]State Key Laboratory of Membrane Biology, Peking University School of Life Sciences, Beijing, China

Correspondence
Marco A. M. Prado and Vania F. Prado, Translational Neuroscience Group, Robarts Research Institute, Schulich School of Medicine & Dentistry, The University of Western Ontario, 1151 Richmond Street North, London, ON N6A 5B7, Canada.
Email: mprado@robarts.ca and vprado@robarts.ca

Funding information
Ontario Graduate Scholarship; Jonathan and Joshua Graduate Scholarship; Fondation Brain Canada (Brain Canada); Gouvernement du Canada | Canadian Institutes of Health Research (CIHR), Grant/Award Number: MOP 126000, MOP 136930, MOP 89919, PJT 162431 and PJT 159781; Gouvernement du Canada | Natural Sciences and Engineering

Abstract

In the striatum, cholinergic interneurons (CINs) have the ability to release both acetylcholine and glutamate, due to the expression of the vesicular acetylcholine transporter (VAChT) and the vesicular glutamate transporter 3 (VGLUT3). However, the relationship these neurotransmitters have in the regulation of behavior is not fully understood. Here we used reward-based touchscreen tests in mice to assess the individual and combined contributions of acetylcholine/glutamate co-transmission in behavior. We found that reduced levels of the VAChT from CINs negatively impacted dopamine signalling in response to reward, and disrupted complex responses in a sequential chain of events. In contrast, diminished VGLUT3 levels had somewhat opposite effects. When mutant mice were treated with haloperidol in a cue-based task, the drug did not affect the performance of VAChT mutant mice, whereas VGLUT3 mutant mice were highly sensitive to haloperidol. In mice where both vesicular transporters were deleted from CINs, we observed altered reward-evoked dopaminergic signalling and behavioral deficits that resemble, but were

Abbreviations: Ach, acetylcholine; ANOVA, two-way analysis of variance; ChAT, choline acetyl-transferase; CIN, cholinergic interneurons; D2, dopamine receptor 2; FR, fixed ratio; GFP, green fluorescent protein; Glu, glutamate; MSN, medium spiny neuron; PR, progressive ratio; RM, repeated measures; SEM, standard error of the mean; VAChT, vesicular acetylcholine transporter; VGLUT3, vesicular glutamate transporter.

Ornela Kljakic and Helena Janíčková should be considered joint first authors.

Research Council of Canada (NSERC), Grant/Award Number: 402524-2013 RGPIN and 03592-2021 RGPIN; Weston Brain Institute; Canada First Research Excellence Fund (CFREF)

worse, than those in mice with specific loss of VAChT alone. These results demonstrate that the ability to secrete two different neurotransmitters allows CINs to exert complex modulation of a wide range of behaviors.

KEYWORDS
acetylcholine, dopamine, glutamate, striatum

1 | INTRODUCTION

The striatum is the principal input structure of the basal ganglia and is involved in regulating a variety of behaviors such as motor function, cognition, motivation, and habit formation.[1,2] The coordination of these roles relies on striatal neurons integrating information received from surrounding brain areas including the cortex, midbrain and thalamus.[2,3] Dysfunction in striatal regulation has been associated with a variety of diseases such as Parkinson's disease,[4,5] Huntington's disease[6,7] and addiction.[8,9] Additionally, recent studies have shown that striatal dysregulation may also correlate with obsessive-compulsive disorder,[10,11] eating disorders,[12,13] schizophrenia,[14,15] and bipolar disorder.[16,17] Therefore, an understanding of how the striatum is regulated is essential to understanding disease and developing treatments.

There is an emerging acceptance that a critical component of the striatal circuitry in both health and disease is cholinergic interneurons (CINs). CINs compose only 2%–3% of all striatal neurons but they represent one of only two sources of acetylcholine (ACh) in the striatum (the other being brainstem cholinergic afferents[18]). CINs are critical for the integration of information processing in the striatum and modulating striatal output.[2,19] CIN signalling has been associated with cognition, movement, reward responses and the regulation of dopamine release.[20–22] ACh release from CINs can have either antagonistic or agonistic effects on dopamine release, depending on the specific striatal subregion and the activity state of local neurons and microcircuits.[23,24] Therefore, to understand the dynamics of striatal dopamine, we need to understand the role played by CINs.

The roles of ACh released by CINs have been studied in various behavioral paradigms, by either lesioning CINs or by using optogenetics and/or chemogenetics to control their activity. However, what is often overlooked is that CINs express both the vesicular acetylcholine transporter (VAChT) and the vesicular glutamate (Glu) transporter 3 (VGLUT3), and thus release both ACh and Glu.[1,25–27] Thus, lesion and activation/inhibition strategies do not disentangle the individual impact of ACh and Glu released by CINs. Importantly, recent studies have indicated that ACh and Glu released by CINs have distinct functions and potentials as therapeutic targets.[1,13,25–29]

In this study, we used three genetically modified mouse lines which have intact CINs but lack either VAChT or VGLUT3 or both transporters (VAChT and VGLUT3, double knockouts) in these neurons. This strategy allows us to examine individual and complementary roles for ACh and Glu released by CINs in reward-evoked dopamine release, response to dopaminergic drugs, and dopamine-dependent behaviors. To investigate complex motor learning and response selection that shows sensitivity to D2 drugs, we adapted for use with mouse touchscreens a heterogeneous sequence test developed by Robbins and collaborators.[30]

2 | MATERIALS AND METHODS

2.1 | Animals

The use and care of the animals was conducted in agreement with the Canadian Council of Animal Care guidelines and the animal protocols approved by the University of Western Ontario (protocols #2016-103, 2016-104). The generation of $VAChT^{flox/flox}$ and $VGLUT3^{flox/flox}$ mutant mouse lines was described previously.[31,32] LoxP sequences flanking the VAChT gene do not interfere with cholinergic marker expression; both $VAChT^{flox/flox}$ and $VGLUT3^{flox/flox}$ mice do not differ from wild-type littermates behaviorally.[31,33] The generation of dopamine receptor 2 (D2)-Cre mice [Tg(Drd2-cre)44Gsat; GENSAT] has been described.[34] D2-Cre mice were backcrossed for at least four generations to C57BL6/J upon arrival to our laboratory. To generate the $VAChT^{D2\text{-}Cre\text{-}flox/flox}$ (VAChTcKO) mouse line, we first crossed $VAChT^{flox/flox}$ (generated as hybrid C57BL/6;129/SvEv and posteriorly backcrossed 10× to C57BL6/J) with D2-Cre mice (obtained from MMRRC as mixed B6/129/Swiss/FVB background, backcrossed 5× to C57BL6/J in our laboratory). Littermates $VAChT^{D2\text{-}Cre\text{-}flox/wt}$ and $VAChT^{flox/wt}$ generated were intercrossed to generate $VAChT^{D2\text{-}Cre\text{-}flox/flox}$ and $VAChT^{flox/flox}$. To generate the $VGLUT3^{D2\text{-}Cre\text{-}flox/flox}$ (VGLUT3cKO) mouse line, we crossed $VGLUT3^{flox/flox}$ (C57BL6/N background) to D2-Cre mice. Littermates $VGLUT3^{D2\text{-}Cre\text{-}flox/wt}$ and $VGLUT3^{flox/wt}$ were intercrossed to generate $VGLUT3^{D2\text{-}Cre\text{-}flox/flox}$ and $VGLUT3^{flox/flox}$. Biochemical and molecular characterization of VAChT and VGLUT3 deletions with the D2-Cre

driver were previously shown (Tables 1 and 2).[13] Double knockout mice (VAChT-VGLUT3$^{D2\text{-}Cre\text{-}flox/flox}$, DKO) were obtained by first intercrossing the VAChT$^{D2\text{-}Cre\text{-}flox/flox}$ mice with VGLUT3$^{flox/flox}$ mice. Cohorts of mice used in the present studies were generated by breeding littermates VAChT$^{D2\text{-}Cre\text{-}flox/flox}$; VGLUT3$^{flox/flox}$ to VAChT$^{flox/flox}$; VGLUT3$^{flox/flox}$.

2.2 | Study design

Studies were performed on 2- to 10-month-old male mice (Table 1). For this initial exploratory work, to understand the behavioral consequences of co-transmission from CINs, we studied male mice given lack of the resources needed to maintain and test larger cohorts that would be necessary to study sex as a biological variable. Three independent cohorts of mutant mice and littermate controls were used to perform different behavioral tasks (Figure 1). Each cohort performed the behavioral tasks once (no technical replicates). Cohort 1 was used to analyze dopamine dynamics, cohort 2 performed touchscreen tasks and cohort 3 performed locomotion.

The *N* values for each group of animals can be found in Figure 1 and in Tables S1–S3. Power analysis was not formally calculated prior to the experiments. Typical sample sizes in experiments using Bussey-Saksida Touchscreen is between 7 and 13 mice per group.[35–38] Based on these previous studies we assigned a minimum of 10 animals per genotype.

Animals were housed in groups of two to four per cage in a temperature-controlled room with a 12:12 light–dark cycle. Food and water were provided *ad libitum* until behavioral testing upon which mice were subjected to mild food restriction (85%–90% of their original weight or 24.5–25.0 g, whichever was lower). While on food restriction, mice were weighed daily, and their weights were kept in a required range. Food-restricted mice were separated and housed individually (due to fighting) or in groups of two per cage. Mice were randomized for behavioral tests and the experimenter was blind to the genotype [following the ARRIVE guidelines[39]]. Experiments were performed between 9 a.m. and 6 p.m. and mice were tested during the light cycle.

2.3 | Quantitative PCR

For mRNA analysis, tissue samples were frozen on dry ice and kept at −80°C until use. RNA was extracted and purified using the Aurum Total RNA Kit (catalog #7326830, Bio-Rad, Mississauga, ON, Canada), according to the manufacturer's instructions. First-strand cDNA was synthesized using the High-Capacity cDNA Transcription Kit (catalog #4368814, Thermofisher Scientific, Waltham, MA, USA) according to the manufacturer's instructions.

TABLE 1 Mouse lines used in this study

Mouse line	Description	Genotype	Littermate control	Reference
VAChTcKO	VAChT deletion in D2 expressing neurons	D2Cre+/−; VAChT$^{flox/flox}$	VAChT$^{flox/flox}$	Guzman et al. 2011[1]; Favier et al. 2020[13]
VGLUT3cKO	VGLUT3 deletion in D2 expressing neurons	D2Cre+/−; VGLUT3$^{flox/flox}$	VGLUT3$^{flox/flox}$	Favier et al. 2020[13]
DKO	VAChT and VGLUT3 deletion in D2 expressing neurons	D2Cre+/−; VAChT$^{flox/flox}$-VGLUT3$^{flox/flox}$	VAChT$^{flox/flox}$-VGLUT3$^{flox/flox}$	This paper

TABLE 2 Expression levels of vesicular transporters in mutant mouse lines as measured with immunoblotting

Protein expression level (% of littermate controls)[a]	VAChTcKO (%)	VGLUT3cKO (%)
Striatum		
VAChT	20	100
VGLUT3	100	10
Hippocampus		
VAChT	100	100
VGLUT3	100	100
Cortex		
VAChT	50	100
VGLUT3	100	100

[a]This is summarized data from matched littermates used in previous D2-Cre studies.[1,13]

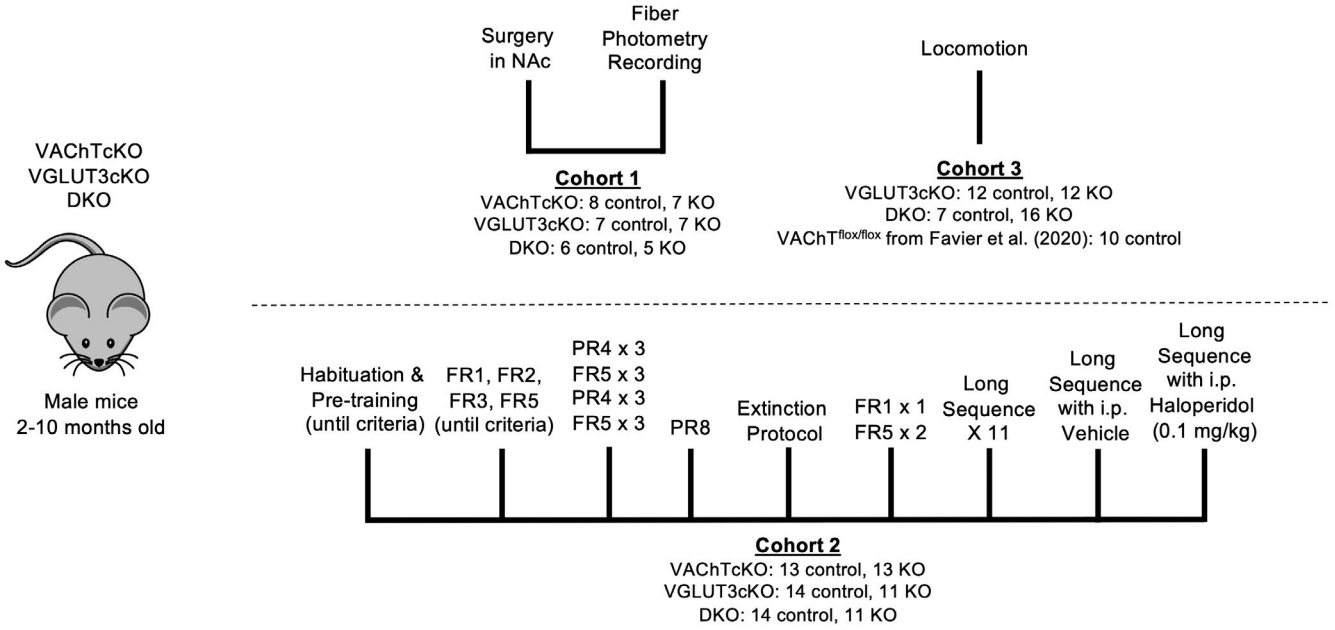

FIGURE 1 Experimental time course

After reverse transcription, the cDNA was subjected to quantitative PCR on a CFX Opus Real-Time PCR System (Bio-Rad) by using SensiFast SYBR Green PCR Master Mix (catalog #BIO-98050, FroggaBio Inc., Concord, ON, Canada) according to the manufacturer's instructions. Relative quantification of gene expression was done with the $2^{-\Delta\Delta Ct}$ method, using β-actin gene expression to normalize the data. The following primers were used to assess mRNA levels. VAChT-F: CCCTTTTGATGGCTGTGA and VAChT-R: GGGCTAGGGTACTCATTAGA, VGLUT3-F: ATTCGGTGCAACCTTGGAGT and VGLUT3-R: TGAAATGAAGCCACCGGGAA, ChAT-F: TTCTGCT GTTATGGCCCTGTGGTA: and ChAT-R: TCAAGATT GCTTGGCTTGGTTGGG. To analyze differences between control ($n = 4$) and KO ($n = 7$) mice, two-tailed unpaired *t*-tests were used.

2.4 | Fiber photometry and dopamine reward response

To assess in vivo dynamics of dopamine in response to reward within the nucleus accumbens shell, real-time fluorescence intensity (V) was recorded using the recently developed D2-based genetically encoded $GRAB_{DA2m}$ dopamine biosensor.[40] Mutant mice (8–20 weeks) and their control littermates were anesthetized using isoflurane administered at a 4%–5% induction rate. Mice were then placed in a stereotaxic frame while anesthesia was maintained at 1.5%–3%. A heating pad was placed under the mice to maintain body temperature (37°C). The top of the skull was exposed and holes were drilled to implant two skull screws and an unilateral microinjection (500 nl, 100 nl/min) of AAV-hSyn.GRABDA2m (3.1×10^{13} gc/ml) at the following coordinates from Bregma (AP: 1.6 mm, ML: 0.3 mm, DV: 3.9 mm).[41] Injectors were left in place for 5 min and then removed slowly. Low-auto-fluorescence optic fiber implants (400 μm O.D, 0.48 NA, Doric Lenses, Quebec City, QC, Canada) were unilaterally inserted just above the injection site.

Prior to experimentation, mice underwent a 4-week recovery period to allow for $GRAB_{DA2m}$ expression within the nucleus accumbens shell. Mice were then food restricted to 85%–90% of their post-recovery body weight to motivate them to perform a simple reward response task using automated touchscreen systems (Lafayette Instruments, Lafeyette, IN, USA). Each trial consisted of the delivery of 2 μl strawberry milkshake (Neilson Dairy, Toronto, ON, Canada) coupled with a 1 s-long tone and a light illuminating the reward magazine receptacle. Mice underwent a total of 20 consecutive trials with pseudo-random inter-trial intervals ranging between 30 and 90 s.

The photometry system was equipped with a fluorescent mini-cube (Doric Lenses) to transmit sinusoidal 465-nm LED light modulated at 572 Hz and a 405-nm LED light modulated at 209 Hz. LED power was set at ~30 μW. Fluorescence from neurons was collected from the optic fiber tip and transmitted back to the mini-cube, amplified and focused into an integrated high sensitivity photoreceiver (Doric Lenses). The signal was demodulated for the brightness produced by the 465-nm excitation (dopamine-dependent $GRAB_{DA}$ fluorescence) versus isosbestic

405-nm excitation (dopamine-independent $GRAB_{DA}$), which allowed for correction from bleaching and movement artifacts. Fluorescent modulated real-time signal from each LED was sampled at 12 kHz and then demodulated and decimated to 100 Hz using Doric Studio (Doric Lenses). For analysis, the least-squares fit was applied to the isosbestic 405-nm signal and used to normalize the 465-nm signal as follows: $\Delta F/F0$ = (465-nm signal—fitted 405-nm signal)/(fitted 405-nm signal). A Time-to-live (TTL, timestamp) output signal (100 ms) from ABET II (Lafayette Instruments) was delivered when mice broke an infrared beam located inside the reward magazine receptacle and it was used to time-lock reward collection with $\Delta F/F0$ dopamine dynamics from the nucleus accumbens. The analysis code used to process the raw fluorescence data is free for download at this link: https://mousebytes.ca/comp-edit?repolinkguid=e46739ed-1154-4d85-bf8c-5cba6b677a74 (Fiber Photometry Analysis Code).

2.5 | Analyses of fiber photometry data

Fluorescent modulated real-time signal from each LED was collected for 20 consecutive reward-delivery trials. The height peak and area under the curve was calculated for each trial. Dopamine responses were then averaged to achieve the final result. To analyze differences between control and KO mice, two-tailed unpaired *t*-tests were used.

2.6 | Immunofluorescence

Once behavioral testing was completed, mice were deeply anesthetized with 100 mg/kg ketamine with 25 mg/kg xylazine, after which they were perfused with ice-cold phosphate-buffered saline followed by 4% paraformaldehyde. The brain from each mouse was then extracted, post-fixed in 4% paraformaldehyde overnight at 4°C, and then transferred to 20% sucrose in phosphate-buffered saline and stored at 4°C prior to sectioning. Coronal sections (30 μm) of the nucleus accumbens were cut using a cryostat (Leica 1950S, Leica Biosystems, Buffalo Grove, IL, USA), and stored in cryoprotectant (2 parts phosphate-buffered saline, 1 part ethylene glycol, 1 part glycerol) at −20°C. For immunofluorescent labelling, the sections were washed three times in phosphate-buffered saline and then blocked for 2 h at room temperature in a solution of phosphate-buffered saline, 0.1% Triton X-100 (PBS-T), 0.1% bovine-serum albumin and 4% normal goat serum (catalog #S-1000, Vector Laboratories, Burlingame, CA, USA). After blocking, the sections were then incubated for 48 h at 4°C with rabbit anti-GFP polyclonal primary antibody conjugated with Alexa Fluor 488 (1:1000, catalog #A-21311, Thermofisher Scientific) diluted in PBS-T, 0.1% bovine-serum albumin and 2% normal goat serum. Sections were then washed three times in phosphate-buffered saline, mounted on to SuperFrost+ slides and cover slipped with Vectashield Vibrance antifade medium with DAPI (catalog #H-1800, Vector Laboratories). Imaging was conducted with an EVOS FL Auto 2 Imaging System (Thermofisher Scientific) to visualize the probe placement and viral-GFP expression on each section.

2.7 | Touchscreen behavioral assessments

All touchscreen-based tasks (fixed ratio-FR and progressive ratio-PR, extinction protocol and the heterogenous sequence task) were conducted using automated Bussey–Saksida Mouse Touchscreen Systems model 81426 (Campden Instruments, Loughborough, England). Schedules were designed and the data were collected using the ABET II Touch software v.2.15 (Lafayette Instruments). As mice were motivated by a food reward (strawberry milkshake, Neilson Dairy), they had to undergo a mild food restriction as described above. For all touchscreen tasks, mice were trained 5 days a week (1 session per day) and each trial required a correct response to be made. In all tasks, the time to press correct window (correct response latency) and time to collect reward (reward collection latency) were measured in addition to other task-specific variables. The order of the touchscreen tasks was as follows: 4 sessions of habituation → pre-training until pre-defined criteria were reached → FR1, FR2, FR3, FR5 until criteria were reached → 3 sessions of PR4 followed by 3 sessions of FR5 for re-baselining and again 3 sessions of PR4 followed by 3 more sessions of FR5 → 1 session of PR8 → Extinction training phase until criteria were reached (minimum 5 sessions) → 6 sessions of Extinction testing phase → 1 session of FR1 followed by 2 sessions of FR5 to ensure renewed performance after extinction → 13 sessions of heterogeneous sequence, the two last sessions with the injection of haloperidol or vehicle as will be further described (see schematic in Figure 1).

2.8 | Habituation and pre-training

Mice were habituated to the touchscreen apparatus at the beginning of the touchscreen-based behavioral testing. The habituation and pre-training procedure are described in detail elsewhere.[42–44] In short, during the habituation, mice were exposed to the touchscreen apparatus for 10–40 min per day and they were gradually habituated to

the milkshake reward with a tone playing whenever the mouse entered the reward magazine.

The habituation was followed by pre-training where the reward was associated with the presentation of a stimulus on the touchscreen. The stimulus appeared randomly in one of the five windows/locations and after 30 s, it was removed, and a reward was given paired with a tone. If the mouse touched the screen while the image was displayed, it immediately received a reward. Once the mouse collected the reward a new trial was initiated. The pre-training session was repeated until the mouse reached the criterion of completion of 30 trials within 60 min for one day. After reaching this criterion (usually within a single session), mice were moved to the Fixed Ratio tasks.

2.9 | Homogeneous tasks: Fixed and progressive ratio tasks

The fixed and progressive ratio tasks (FR and PR, respectively), which assess operant responding were performed as described by Heath et al. (2016) with slight modifications.[45] Both are homogeneous touchscreen tasks that rely on mice emitting multiple touches on the same grid to receive a reward (in contrast to heterogenous tasks that require touches across different grids). In both the FR and PR tasks, trials were not required to be initiated by magazine entrance and started automatically after a 5 s inter-trial interval. Each response in both the fixed and progressive ratio tasks was accompanied by a short click-like tone. If the required number of responses was reached, the reward tone was played, the reward was delivered into the illuminated magazine and the stimulus was removed from the screen for 500 ms.

In the FR tasks, mice were required to make a fixed number of responses (nose-pokes) to a white square stimulus located in the center of the screen in order to get a reward. The number of required responses ranged from 1 to 5 and always stayed the same in a given session. Testing was initiated with a session where only one response was required (FR1) and after reaching criterion (completing 30 trials in 60 min for two consecutive days) the mice were transferred to a session with a more demanding number of responses (FR2, FR3 and FR5). The criterion in the more demanding protocols was the same as in FR1 (completing 30 trials in 60 min) except only one day of reaching this criterion was required. The mice were moved through the task based on their own level of performance (not influenced by performance speed of littermates) to ensure they did not get overtrained in the task. Performance was analyzed for the first session of each fixed ratio stage (e.g., if the mouse required 3 sessions to reach FR5 criteria, session 1 was used for analysis). After reaching criterion in the last FR session, the mice were transferred to the progressive ratio (PR) task.

In the PR task, the number of responses required to obtain the reward was actively increasing during a single session. In every new trial, the number of responses required was increased by 4 during a single session (PR4, so the number of responses was 4, 8, 12, 16 etc. in the session). The PR session was terminated automatically after 60 min or after 5 min of inactivity (no response was made and no magazine entry). Mice underwent three consecutive sessions of the PR task followed by three sessions of FR5 (re-baseline) and by another 3 sessions of the PR task and then three sessions of FR5. After that, one session of the more demanding PR8 task was introduced, where the required number of responses progressively increased by 8 within a single session. The maximum trials mice were willing to perform (breakpoint) was analyzed for all PR4 and PR8 sessions.

2.10 | Extinction procedure

Following the completing of the homogenous tasks (FR/PR), the extinction task was used to dissociate center window pressing from reward. A protocol described by Nithianantharajah et al. (2013) was followed with minor modifications.[46] During the extinction training phase, mice were required to respond to a white square stimulus presented in the center of the screen in order to obtain a reward. The stimulus remained on the screen until a response was made and was removed afterwards together with the appearance of a tone, magazine illumination and reward delivery. The training criterion was defined as completing 30 trials within 12.5 min for five consecutive sessions. After reaching this criterion, mice were transferred to an extinction probe phase in which responses to the stimulus were no longer rewarded nor accompanied by any other feedback. During the probe sessions, the stimulus was displayed for 10 s and then it was automatically removed if a response was not made. After a 10 s inter-trial interval, a new trial (stimulus presentation) was automatically initiated. The session was terminated after 30 trials (maximum time of 1 session when no response was made was 12.5 min). The extinction probe phase was conducted over the course of six days (one session per day).

2.11 | Heterogenous sequence task

To better understand operant responding in mutant mice, we modified the protocol of the heterogeneous sequence task as described by Keeler et al. (2014)[30] and adapted it for touchscreens (see Janickova, Kljakic et al. 2021).[47] Similar to the FR and PR tasks, mice had to respond a

white square stimulus multiple times in order to get a reward. However, in the heterogeneous sequence task, the stimulus was presented sequentially in five different locations on the screen from the left to the right, so mice were required to make five sequential responses, each to one of the five windows. As the stimulus appeared in a row from the left to the right side of the screen, the distance between two successive stimuli was always identical. A correct response to each location was accompanied by a short click-like tone and the stimulus disappeared for 500 ms. After the final response was made to the fifth location, the mouse was required to enter the magazine after which the reward tone was played, and the reward was delivered. Every new trial was automatically initiated 5 s after reward collection (5 s inter-trial interval) and a maximum of 30 trials could be completed within 60 min in each session. This was performed for 11 consecutive days after which the mice underwent treatment before performing the heterogeneous sequence sessions. On days 12 and 13, mutant mice and littermate controls were intraperitoneally injected with vehicle (0.2% lactic acid) or D2 antagonist haloperidol (0.1 mg/kg), respectively, 30 min prior to testing in the touchscreens. Haloperidol (catalog #H1512, MilliporeSigma, Oakville, ON, Canada) was dissolved in 0.2% lactic acid.

2.12 | Locomotor activity

Locomotor activity was measured in an open field arena (20 cm × 20 cm platform with 30 cm high walls) as previously described[31] and movement in the arena was recorded by AccuScan Instruments Inc. (Columbus, OH). Mice were placed in the centre of the apparatus and allowed to freely explore the novel environment for 120 min during the light phase (between 9 a.m. and 5 p.m.). For intersession habituation, mice spent 120 min in the same open field apparatus for three consecutive days. Total distance travelled (converted from beam breaks to cm) was calculated at 5-min intervals. VAChT$^{flox/flox}$ control locomotor data has been previous published in Favier et al., 2020—fig. S7N.[13] It was used here only to compare general exploration for the three control mouse lines used in the experiment. To analyze differences between control and KO mice, two-way repeated measures ANOVA with Sidak's multiple comparisons post-hoc test was used.

2.13 | FR analyses

In all FR stages (FR1, FR2, FR3, and FR5) the time it took to complete 30 trials in the first session was analyzed to evaluate differences in learning of the operant task. Several parameters were analyzed during the same session: Number of Blank Touches—touches on non-illuminated windows; Correct Response Latency—reaction time for correct response; Reward Collection Latency—reaction time to collect the reward on correct trials. To analyze differences between control and KO mice, two-way ANOVA with Sidak's multiple comparisons post-hoc test or two-tailed unpaired *t*-tests were used (a repeated measures ANOVA was only used for FR1 time to complete task).

2.14 | PR analyses

In the PR stages, the breaking point (maximum trials mice were willing to perform) was used to analyze motivation. Several parameters were analyzed during the same session: Number of Blank Touches—touches on non-illuminated windows; Correct Response Latency—reaction time for correct response; Reward Collection Latency—reaction time to collect the reward on correct trials. To analyze differences between control and KO mice, two-way repeated measures ANOVA with Sidak's multiple comparisons post-hoc test or two-tailed unpaired *t*-tests were used.

2.15 | Heterogenous sequence analyses

In all heterogenous sequence sessions, the time it took to complete 30 trials was analyzed to evaluate differences in learning of the operant task. Other parameters were analyzed across the same sessions: Number of Blank Touches—touches on non-illuminated windows; Reward Collection Latency—reaction time to collect the reward on correct trials. Slowing factor was also analyzed on the last sequence session (Day 11). Initiation Factor was calculated as a ratio of correct response latency Grid 1 ÷ control average correct response latency Grid 1. Termination Factor was calculated as a ratio of reward collection latency ÷ control average reward collection latency. To analyze differences between control and KO mice, two-way repeated measures ANOVA with Sidak's multiple comparisons post-hoc test was used (a non-repeated measures ANOVA was only used for blank touches across grids).

For drug test days, performance in one session of the heterogeneous sequence task was assessed. Performance speed was calculated as correct trials completed over a specific time window. The rest of the task parameters were calculated as a ratio of haloperidol performance ÷ vehicle performance: Time to Complete Task, Number of Blank Touches—touches on non-illuminated windows (total and per grid); Correct Response Latency—reaction

time for correct response per grid. Slowing factor was also analyzed for the drug sessions. Initiation Factor was calculated as a ratio of correct response latency Grid 1 haloperidol session ÷ correct response latency Grid 1 vehicle session. Termination Factor was calculated as a ratio of reward collection latency haloperidol session ÷ reward collection latency vehicle session. To analyze differences between control and KO mice, two-way repeated measures ANOVA with Sidak's multiple comparisons post-hoc test or two-tailed unpaired *t*-tests were used (a non-repeated measures ANOVA was only used for blank touches and correct response latency across grids). One VAChTcKO control mouse ($VAChT^{flox/flox}$) did not receive the proper dose of haloperidol so was excluded from analysis of drug test days.

2.16 | Statistical analysis

All collected data were statistically analyzed and graphed using GraphPad Prism 8.0. Data were plotted as mean ± SEM. Normality was evaluated with the D'Agostino & Pearson test when comparing two datasets (a Shapiro-Wilks normality test was only used for the photometry data as the *n*-value was low). A Student's *t*-test was used for comparisons between two experimental groups and a two-way analysis of variance (ANOVA) was conducted to compare several treatment groups. For tasks that included more than one session, ANOVA with repeated measures (RM) was used. If data did not pass normality, a Mann-Whitney test was performed. A Sidak's post hoc test was used wherever appropriate. p Values $< .05$ were considered as statistically significant. Touchscreen data on latencies were evaluated for irregularities. In particular, large high value correct response latencies and 0 s reward collection latencies are often a result of software errors. Any latency value beyond Average ± 3 (Standard Deviations) was automatically removed from the dataset. These data were then analyzed with a mixed-effects test. The same outlier formula was used to evaluate the rest of the touchscreen parameters. Full statistical tables are provided for all data (Tables S1–S3), with main parameters also described in the text.

3 | RESULTS

3.1 | Mice with a striatal knockout of VAChT or VGLUT3

To be able to assess the impact of co-transmission from CINs of the striatum we used the Cre-LoxP approach to selectively delete the vesicular transporters for ACh and Glu. To target striatal CINs but leave other populations of cholinergic neurons intact, we chose the promoter for the D2 receptor as the Cre driver (Table 1). Choline acetyl-transferase (ChAT)-Cre was not used as the Cre driver since crossing ChAT-Cre mice with $VAChT^{flox/flox}$ mice would silence VAChT in all cholinergic neurons of the body, including motor neurons causing respiratory paralysis. Notably, global homozygous VAChT-KO mice have a major muscular deficit and die shortly after birth[48] and even selectively targeting VAChT in motor neurons causes weakness and death after few months.[49] D2-Cre avoids this problem but still retains some precision with transporter deletion as it is highly expressed on striatal CINs and also allows for the use of the same Cre driver for the double knockout mice. Specifically, we previously established, using in situ hybridization and immunoradiography, that using D2-Cre as a driver targets transporter expression in the striatum but not in the pedunculopontine or motor nuclei of the brainstem.[1,13] We also demonstrated that D2-Cre expression by itself does not induce striatal-dependent behavioral phenotypes.[1,13] Furthermore, we previously evaluated how D2-Cre affects the loss of VAChT and VGLUT3 expression in different brain regions of VAChTcKO and VGLUT3cKO mice using immunoblotting (see summary in Table 2).[1,13] In particular, VAChT and VGLUT3 expression is almost completely abolished in the striata of the respective lines. Assessment of striatal-specific vesicular transporter expression levels showed the greatest degree of decrease in the dorsal striatum (see summary in Table 3).[13] Examination of DKO mice, revealed a significant decrease in striatal expression of VAChT mRNA (Figure S1A; unpaired *t*-test: $t(9) = 5.685$, $p = .0003$) and VGLUT3 mRNA (Figure S1B; unpaired *t*-test: $t(9) = 3.749$, $p = .0046$), yet no changes in

TABLE 3 Striatal-specific expression levels of vesicular transporters in mutant mouse lines as measured with immunoautoradiography

	VAChTcKO[a]	VGLUT3cKO[a]
Striatal subregion	**VAChT expression (% of littermate controls)**	**VGLUT3 expression (% of littermate controls)**
Nucleus accumbens	~50	~70
Dorsomedial striatum	~20	~20
Dorsolateral striatum	~20	~15

[a]This is summarized data from matched littermates used in previous D2-Cre studies.[13]

ChAT mRNA levels (Figure S1C). Notably, using D2-Cre to solely delete VAChT does not cause changes in mRNA and protein expression of VGLUT3 and vice versa.[13] Consequently, we focused on behaviors that are known to be striatal specific (behavioral tasks are depicted in Figure 1).

Previous experiments have characterized ACh[1,13] and dopamine release using microdialysis and amperometry[13,50] in VAChT and VGLUT3 deficient mice. VAChT and VGLUT3 deletions differentially affect KCl-induced dopamine release in the striatum of anesthetized animals.[13,50] To determine if in freely behaving mice dopamine signalling is also differentially affected by the elimination of VAChT or VGLUT3, we transduced the genetic-encoded dopamine sensor, $GRAB_{DA2m}$ into the nucleus accumbens shell of mutant mice and their littermate controls using a viral vector (see schematic Figures 2A and S2). The $GRAB_{DA2m}$ is a GPCR-D2 based biosensor that allows for real-time detection of dopamine dynamics.[40] As dopamine neurons strongly fire in response to reward, we used reward delivery (provided in a touchscreen reward magazine receptacle when a 1 s-long tone was played) to elicit dopamine signalling in the nucleus accumbens. Notably, it has been demonstrated that reward collection leads to a phasic increase of extracellular dopamine levels in the nucleus accumbens.[51,52] We found that when reward was elicited, mice immediately moved towards the magazine receptacle, and as the task progressed, they spent more time sitting in front of the port, waiting for reward to be delivered at a pseudo-random intertrial duration (30–90 s).

Control mice and VAChTcKO mice demonstrated an increase in reward-evoked dopamine response that lasted 5 s (Figure 2). However, VAChTcKO mice presented a smaller peak (Figure 2C; unpaired *t*-test: $t(13) = 2.980$, $p = .0106$) and the overall level of response was lower (area under the curve, Figure 2D; unpaired *t*-test: $t(13) = 5.401$, $p = .0001$) compared to controls. In VGLUT3cKO mice the dopamine peak height was not significantly different between VGLUT3cKO mice and controls (Figure 2E,F). However, the duration of the peak as well as the total amount of dopamine signal (estimated by the area under the curve) was significantly higher in VGLUT3cKO mice compared to littermate controls (Figure 2G; unpaired *t*-test: $t(12) = 2.868$, $p = .0141$).

To determine the consequences that arise when CINs are completely silenced in their ability to release either ACh or Glu, we used VAChT and VGLUT3 double KO mice (DKO, Table 1).

Interestingly, the reward-evoked dopamine response in DKO mice presented a combination of characteristics observed in both VAChTcKO and VGLUT3cKO mice (Figure 2H). That is, similar to VAChTcKO mice, DKO mutants had a lower height of signal peak (Figure 2I; unpaired *t*-test: $t(9) = 2.714$, $p = .0238$). However, they do not differ in area under the curve compared to littermate controls (Figure 2J); this is because, similar to VGLUT3cKO mice, they show a lingering dopamine response. We also evaluated $VAChT^{flox/flox}$-$VGLUT3^{flox/flox}$ (control) mice and found that similar to the other control lines ($VAChT^{flox/flox}$, $VGLUT3^{flox/flox}$) they had an increase in reward-evoked dopamine response that lasted 5 s (Figure 2). These three control lines did not differ in height peak (data not shown, One-way ANOVA; main effect of genotype: $F(2,18) = 0.03329$, $p = .9673$) nor area under the curve (data not shown, One-way ANOVA; main effect of genotype: $F(2,18) = 0.9781$, $p = .3951$). To note, for all investigated genotypes we found no significant differences in the reward responses across time (data not shown, 50–70 reward collection trials/mouse). Taken together, these results suggest that CIN-expressed VAChT and VGLUT3 differentially modulate reward-evoked dopamine signalling in freely moving mice.

3.2 | DKO mice show a learning impairment in the initial phase of the fixed ratio touchscreen task

To determine how the absence of VAChT or VGLUT3 from CINs affects striatal-modulated behaviors, we tested VAChTcKO, VGLUT3cKO and DKO mice in a battery of reward-based operant touchscreen tasks (see schematic in Figure 1). In these tasks, mice had to perform multiple touches to either the same or different touchscreen grids, referred to as either homogeneous (FR, PR task) or heterogeneous sequence tasks, respectively, see also Keeler et al. (2014).[30] We first evaluated mice in the fixed ratio (FR) task, where mice had to press a central illuminated window a fixed number of times to receive a reward (Figure 3A). We found that the performance of VAChTcKO mice did not significantly differ from littermate controls in terms of time to complete trials, touches on non-illuminated windows (blank touches), time to press correct window (correct response latency) and time to collect reward (reward collection latency, Figures 3 and S3). This suggests VAChTcKO mice do not struggle completing this simple operant task.

VGLUT3cKO mice also did not significantly differ from controls in the FR1 session (FR1, Figures 3 and S3). However, these mutant mice performed the more demanding FR sessions faster (Figure 3H; Two-way ANOVA; main effect of genotype: $F(1,69) = 10.45$, $p = .0019$), measured as a decrease in blank touches (Figure 3I; Two-way ANOVA; main effect of genotype: $F(1,69) = 5.154$, $p = .0263$) and a shorter correct response latency (Figure S3G; Two-way ANOVA; main effect of genotype:

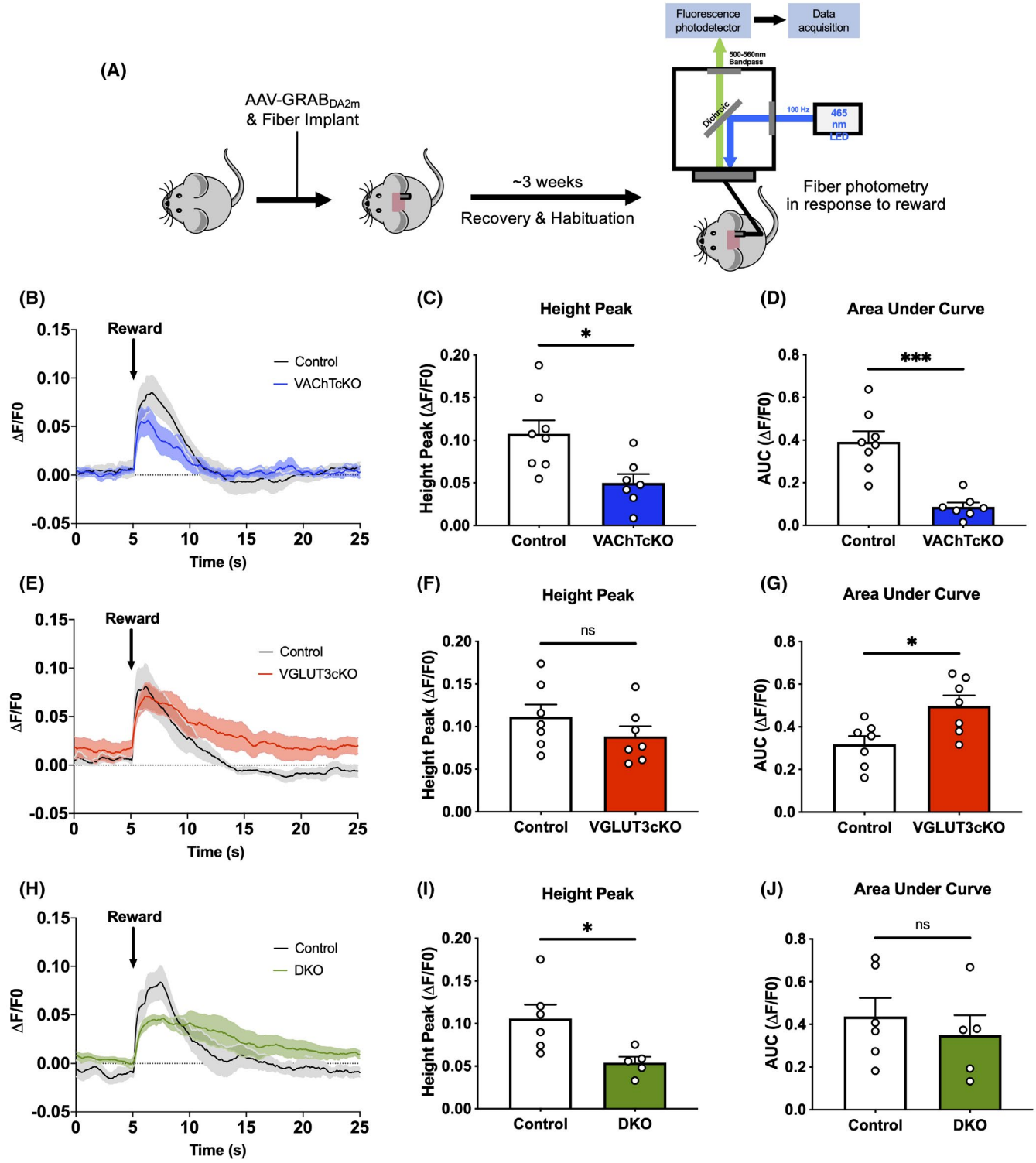

FIGURE 2 ACh and Glu released by CINs have opposing effects on dopamine response to reward. (A) Schematic of dopamine recording. (B–J) Dopamine parameters recorded in response to reward: (B, E, H) overall signal change, (C, F, I) height of the signal peak and (D, G, J) area under the curve. Data are expressed as mean ± SEM, *$p < .05$, ***$p < .001$. Summary statistics in Table S1

$F(1,68) = 7.556$, $p = .0077$). Although, no change was detected in reward collection latency (Figure S3H). Together, these results suggest that the faster completion of the task by VGLUT3cKO mice compared to their littermate controls is not caused by their higher motivation to obtain a reward but rather by increased responsiveness to the reward-related cue (i.e., illuminated position in the touchscreen, with decreased blank touches).

DKO mice, which had both VAChT and VGLUT3 deleted from CINs, were also assessed in the same FR tasks.

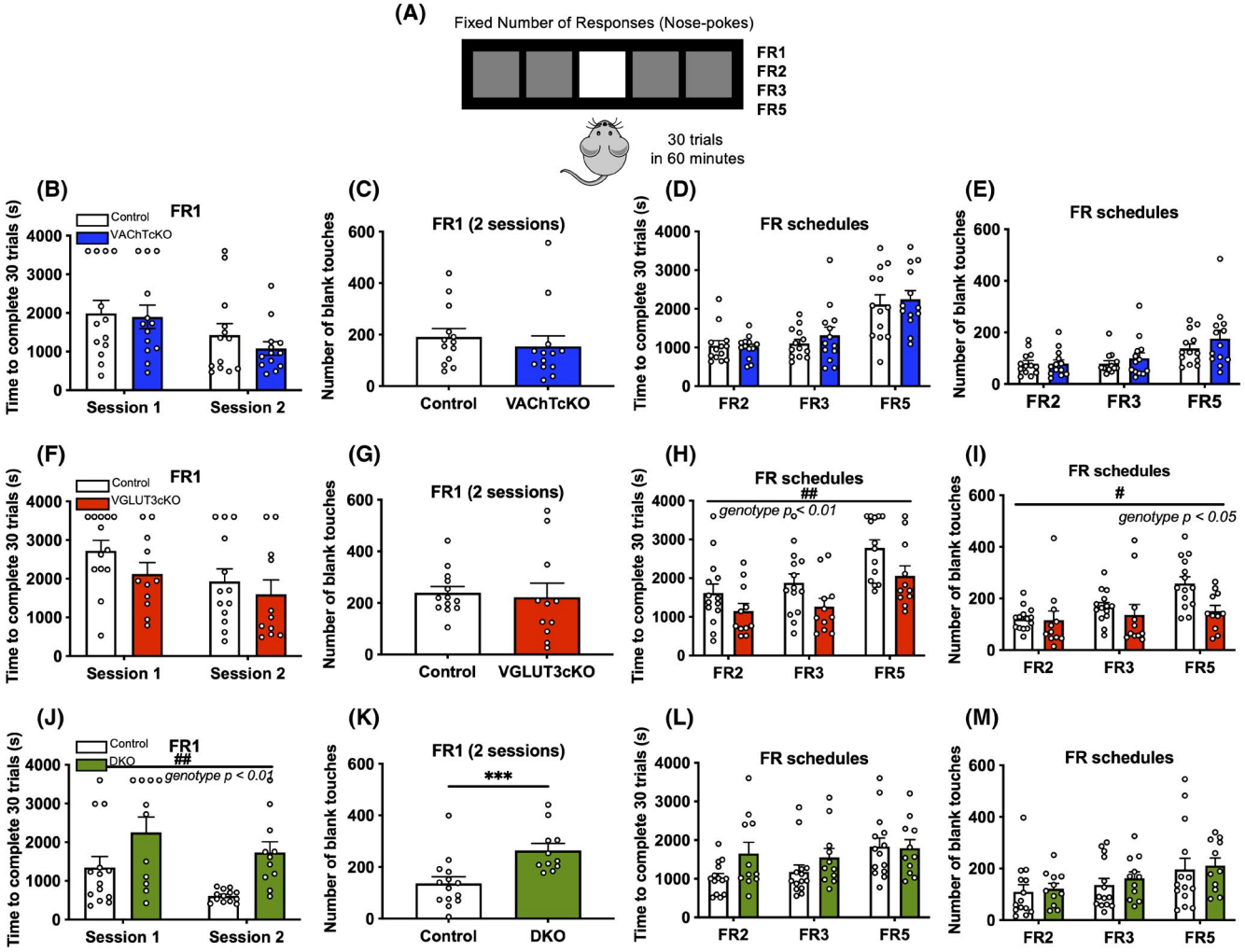

FIGURE 3 DKO mice have a learning impairment in the initial fixed ratio task sessions. (A) Schematic of the fixed ratio touchscreen task: mice are required to make a fixed number of responses (nose-pokes) to a white square stimulus located in the center of the screen to receive a reward. (B–M) Parameters recorded during the fixed ratio touchscreen tasks: (B, F, J) time to complete 30 trials for FR1, (C, G, K) number of blank touches for FR1, (D, H, L) time to complete 30 trials for FR2, FR3 and FR5 and (E, I, M) number of blank touches for FR2, FR3 and FR5. Data are expressed as mean ± SEM, $^{\#}p < .05$, $^{\#\#}p < .01$, $^{\#\#\#}p < .001$. Summary statistics in Table S2

We found that DKO mice were initially slower than wild-types controls to learn the FR task (FR1) (Figure 3J; Mixed effect model; main effect of genotype: $F(1,23) = 8.195$, $p = .0088$) but improved to wild-type levels as training continued (FR3, FR5) (Figure 3L; Two-way ANOVA; main effect of genotype: $F(1,69) = 3.565$, $p = .0632$). The impaired performance in FR1 was accompanied by an increased number of blank touches (Figure 3K; Mann–Whitney test: $U = 18$, $p = .0007$), longer correct response latency (Figure S3I; Mann–Whitney test: $U = 15$, $p = .0011$) and reward collection latency (Figure S3J; unpaired t-test: $t(23) = 3.328$, $p = .0029$). During FR2-5 training days, there were changes in correct response latency (Figure S3K; Two-way ANOVA; main effect of genotype: $F(1,68) = 4.519$, $p = .0372$) and reward collection latency (Figure S3L; Two-way ANOVA; main effect of genotype: $F(1,68) = 4.999$, $p = .0287$) but not in the number of blank touches (Figure 3M). These results suggest that DKO mice struggle to initially learn an action-outcome association, but as training is prolonged they managed to reach the levels of their control mice.

Surprisingly control lines showed differences in operant performance suggesting that a slight difference of genetic background in the three lines seems to affect performance in this task. Since their reward collection latencies were similar across all fixed ratio tasks (data not shown, FR1-5: Two-way ANOVA; main effect of genotype: $F(2,149) = 0.2757$, $p = .7594$), the impact of the genetic differences seems specific to the task parameters. This observation argued for the evaluation of the performance of mutant mice based on comparisons with their littermate controls. To note, the period at which the task was run could also lead to some variability, as groups of mice were evaluated in different timeframes, due to our limited capacity to test all groups

simultaneously (however, mutant mice were always tested concurrently with their respective littermate controls).

3.3 | DKO mice show an increased rate of responding during the progressive ratio task

We next evaluated motivation using the progressive ratio (PR) touchscreen task where to receive a reward, mice had to press a central illuminated window a number of times that was incrementally increased each trial (Figure 4A). Both VAChTcKO and VGLUT3cKO mice did not differ from their respective littermate controls in both PR4 and PR8 (Figures 4 and S4). VAChTcKO and VGLUT3cKO mice did not differ in maximum trials they were willing to perform (breakpoint), blank touches, correct response latency and reward collection latency in both PR4 and PR8. This supported the notion that the motivation is not altered in these two mutant mouse lines.

Notably, we found that DKO mice had a higher breakpoint in PR4 (Figure 4J; Two-way RM ANOVA; interaction effect of time × genotype: $F(5,115) = 2.963$, $p = .0149$) and in the more demanding PR8 (Figure 4L; unpaired t-test: $t(21) = 3.399$, $p = .0027$) compared to littermate controls. Interestingly, the increased motivation was not observed at the beginning of the task and only appeared after two days of training in PR4. On the third day, while the

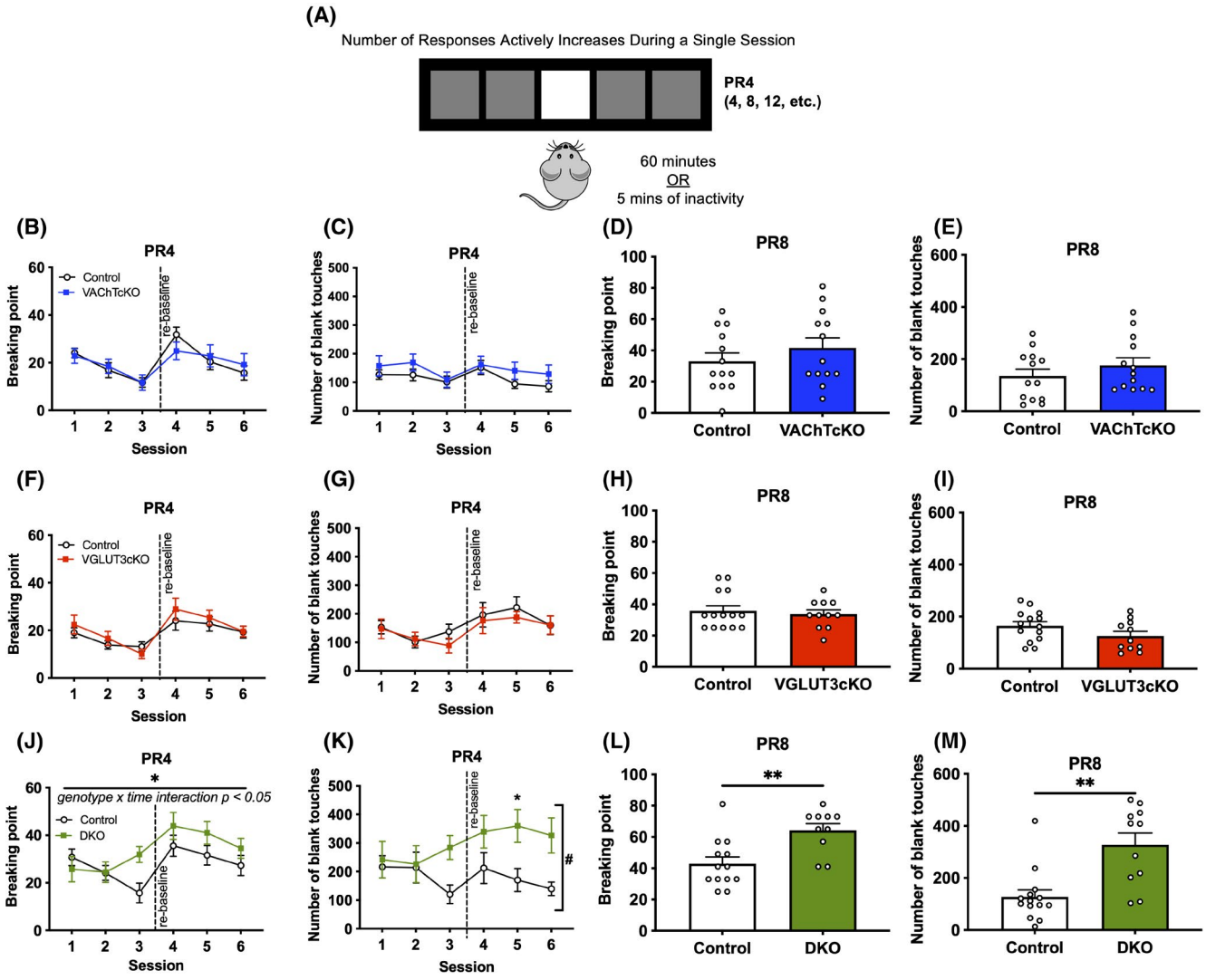

FIGURE 4 DKO mice have higher responding during the progressive ratio tasks. (A) Schematic of the progressive ratio touchscreen task: mice are required to make responses (nose-pokes) that are actively increasing in a single session, on a white square stimulus located in the center of the screen to receive a reward. (B–M) Parameters recorded during the progressive ratio touchscreen tasks: (B, F, J) breaking point (maximum trials mice were willing to perform) in PR4, (C, G, K) number of blank touches in PR4, (D, H, L) breaking point in PR8 and (E, I, M) number of blank touches in PR8. Data are expressed as mean ± SEM, *comparing to matched littermate control parameter, #overall genotype effect, *$p < .05$, **$p < .01$. Summary statistics in Table S2

performance of control mice decreased, the mutants' performance developed in the opposite direction (Figure 4J). This might suggest that the DKO mice are more prone to developing habitual behavior (nose-poking) rather than showing higher motivation. The higher breakpoint in PR tasks was accompanied by an increased number of blank touches (Figure 4K; Two-way RM ANOVA; main effect of genotype: $F(1,23) = 5.804$, $p = .0244$; Figure 4M; Mann–Whitney test: $U = 21$, $p = .0014$), but no change in reward collection latency (Figure S4J,L). The correct response latency was also decreased in DKO mice during two particular sessions of the PR4 training while later it matched the control values (Figure S4I,K).

Prior to performing more touchscreen tasks, we extinguished center pressing behavior using an extinction touchscreen task to ensure overtraining would not bias future results. We found that all experimental mice extinguished center pressing and did so to a similar degree (Figure S5A; Two-way RM ANOVA; main effect of task session: $F(1,140) = 7050$, $p < .0001$).

3.4 | Sequential learning is influenced by striatal VAChT

We next assessed response chain learning and complex motor learning using the heterogenous sequence task.[30] Mice were trained to press five grids sequentially in the touchscreen, from left to right, to receive a reward for 11 sessions (Figure 5A). Early (left) components are

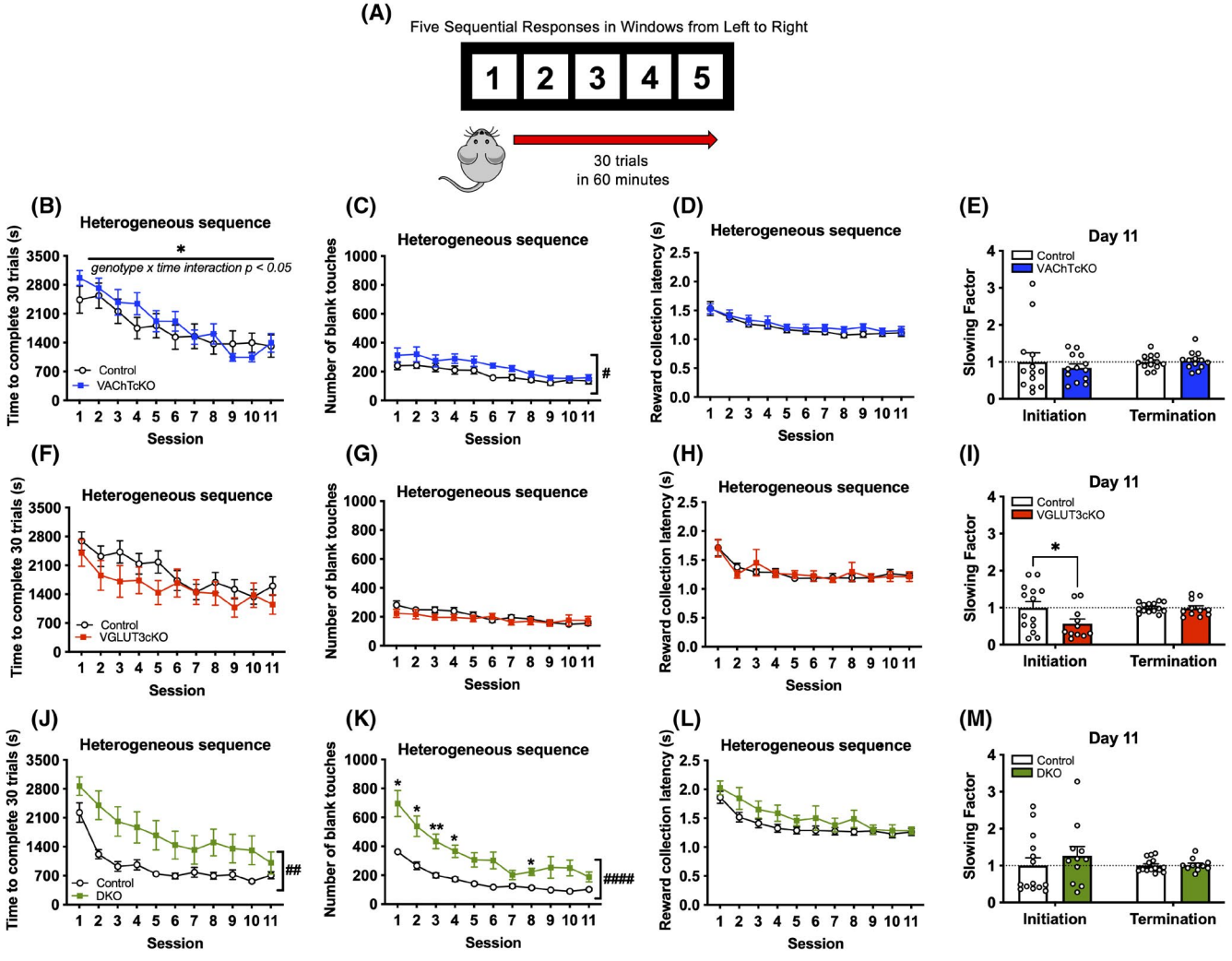

FIGURE 5 ACh and Glu released by CINs have opposing effects on the speed at which the heterogeneous sequence task is completed. (A) Schematic of the heterogeneous sequence task: mice are required to make a five sequential responses (nose-pokes) from left to right on a white square stimulus to receive a reward. (B–M) Parameters recorded during the heterogenous sequence touchscreen task: (B, F, J) time to complete 30 trials, (C, G, K) number of blank touches, (D, H, L) reward collection latency and (E, I, M) slowing factor during the initial and final steps of the sequence (speed at which task was started versus ended as a ratio of control latency). Data are expressed as mean ± SEM, *comparing to matched littermate control parameter, #overall genotype effect, *$p < .05$, **$p < .01$, ****$p < .0001$. Summary statistics in Table S2

considered distal to reward with late ones (right) proximal to reward. Of note, the correct grids to be pressed were always sequentially highlighted on the screen, thus creating light cues that mice could follow. We found that VAChTcKO mice took longer to complete this task compared to their littermate controls, especially at the beginning of training (Figure 5B; Two-way RM ANOVA; interaction effect of time × genotype: $F(10,240) = 1.880$, $p = .0486$). This slower performance was accompanied by a significant change in the number of blank touches in VAChTcKO mice as they did more nose-pokes on non-highlighted locations than controls (Figure 5C; Two-way RM ANOVA; main effect of genotype: $F(1,24) = 4.566$, $p = .0430$). Reward collection latency was not changed in VAChTcKO mice (Figure 5D). Together these results indicate that motivation to perform the task was not altered, yet mutant mice had difficulties following the sequential cues. Nonetheless, VAChTcKO mice were able to improve during training. After 11 days of training, VAChTcKO mice responded as quickly as controls (slowing factor) to both the reward-distal (Initiation: Grid 1) and reward-proximal (Termination: Reward Magazine) components (Figure 5E: response latency to component/average control response latency).

VGLUT3cKO mice showed little alteration in performance compared to their littermate controls. They did not differ in blank touches (Figure 5G) and reward collection latency (Figure 5H). Nonetheless, VGLUT3cKO mice did show a non-significant trend to be quicker to perform the task during early sessions (Figure 5F; comparison first 5 sessions: Two-way RM ANOVA; main effect of genotype: $F(1,23) = 3.999$, $p = .0575$). However, loss of VGLUT3 in CINs selectively and significantly sped up performance of early sequence components (Grid 1 correct response latency) but left final components unaltered after 11 days of training (Figure 5I; Two-way RM ANOVA; main effect of genotype: $F(1,23) = 3.915$, $p = .06$, post hoc Sidak test: Initiation, $p = .0203$). This finding suggests that VGLUT3cKO mice have a better recognition of distal cues.

DKO mice, on the other hand, were slower to complete the heterogeneous sequence task when compared to their respective controls (Figure 5J: Mixed-effects model; main effect of genotype: $F(1,23) = 7.7889$, $p = .01$) and made significantly more blank touches compared to littermate controls (Figure 5K: Mixed-effects model; main effect of genotype: $F(1,23) = 23.61$, $p < .0001$). This change in performance was not accompanied by an increased reward collection latency (Figure 5L). Furthermore, neurochemical silencing of CINs did not affect performance in early and late sequence components after 11 days of training (Figure 5M). Overall, these behavioral changes reproduce what we observed with VAChTcKO mice.

Similar to the homogenous sequence tasks we saw differences in the speed of performance of control mice across genotypes in the heterogeneous sequence task which we need to consider. Controls from DKO mice were much faster than the other two control mice and seem to make more blank touch mistakes. Nonetheless, reward collection latency was similar between all controls, suggesting that the difference in DKOs is meaningful (data not shown, Two-way RM ANOVA; main effect of background: $F(2,38) = 2.301$, $p = .1139$). Furthermore, to determine if the changes in performance speed during the heterogenous task might be related to a more general hyper or hypoactive phenotype, we examined the performance of mice in locomotor boxes. Using VAChT$^{flox/flox}$ control data from our previous publication, Favier et al. (2020), we first compared locomotor activity of the three controls' lines.[13] We find that control mice across the three lines do not differ in their exploration nor habituation in locomotor boxes (Figure S5B), further suggesting that the observed behavioral differences of mutant mice are meaningful.

In multiple previous papers, we have shown that VAChTcKO mice do not differ in locomotor activity compared to littermate controls (both in exploration and habituation).[1,13,29,53] In contrast, we found that VGLUT3cKO mice are hyperactive but can still habituate to the boxes (Figure S5C; Two-way RM ANOVA; main effect of genotype: $F(1,22) = 11.04$, $p = .0031$), somewhat similarly to global VGLUT3-KO mice.[50] Notably, similar to VGLUT3cKO mice, DKO mice are also hyperactive but can habituate to their environment (Figure S5D; Two-way RM ANOVA; main effect of genotype: $F(1,21) = 8.388$, $p = .0086$).

3.5 | Striatal VAChT and VGLUT3 have dissociative effects on responses to haloperidol

The performance of rodents in the heterogenous sequence task is highly dependent on dopaminergic function, specifically D2 receptors.[30] To further examine whether DKO mice present features that may be related to loss of VAChT or VGLUT3, and given the bimodal regulation of dopamine release operated by CINs,[13,50] we tested the sensitivity of touchscreen performance of both mutant lines to the D2 antagonist haloperidol. A low dose of haloperidol (0.1 mg/kg) was previously shown to affect motivated behavior without inducing catalepsy in rodents.[54] Notably, Keeler et al. (2014) demonstrated that the ability to complete a heterogeneous sequence is inhibited by a low dose of D2 antagonist (sulpride).[30] Consequently, mutant mice and their

littermate controls were intraperitoneally treated with haloperidol (0.1 mg/kg) and assessed in the heterogenous sequence task for one session. In comparison to vehicle treatment, all three control mouse lines treated with haloperidol showed a slower speed of performance (Figure 6A; Two-way RM ANOVA; main effect genotype: $F(1,23) = 7.631$, $p = .0111$, Figure 6D; Two-way RM ANOVA; main effect genotype: $F(1,26) = 3.350$, $p = .0787$; Figure 6G; Two-way RM ANOVA; main effect of genotype: $F(1,26) = 12.78$, $p = .0014$) and took twice as long to complete the task (haloperidol/vehicle ratio =2; Figure 6B,E,H). This was accompanied by the absence of changes in the overall number of blank touches, but an increased correct response latency across early grids (haloperidol/vehicle ratio > 1; Figure S6). In controls, haloperidol selectively and significantly slowed the performance of early sequence components (initiation: ~3-fold increase) but did not show any effect on the final components (termination) (Figure 6C,F,I).

In contrast, the performance of VAChTcKO mice was not significantly affected by haloperidol treatment. VAChTcKO mice treated with haloperidol completed the task as quickly as when they were treated with vehicle (Figure 6A,B). This was accompanied by no change in the overall number of blank touches (Figure S6A,B) and correct response latency (Figure S6C). Notably, while haloperidol slowed down task initiation in control mice, VAChTcKO mice were unaffected (Figure 6C).

The performance of VGLUT3cKO mice after haloperidol administration was comparable to control mice treated with the drug. In comparison to vehicle treatment, VGLUT3cKO mice treated with haloperidol had slowed performance (Figure 6D; Two-way RM ANOVA; main effect of genotype: $F(1,20) = 9.365$, $p = .0062$, Figure 6E) that was accompanied by no change in the overall blank touches but an increased correct response latency across all grids (Figure S6D–F). Notably, haloperidol slowed down task initiation in the VGLUT3cKO mice. That is, when treated with haloperidol VGLUT3cKO mice took ~5× longer to initiate the task than when they were treated with vehicle (initiation slowing factor = 5.6, Figure 6F). This effect was specific to the early sequence components

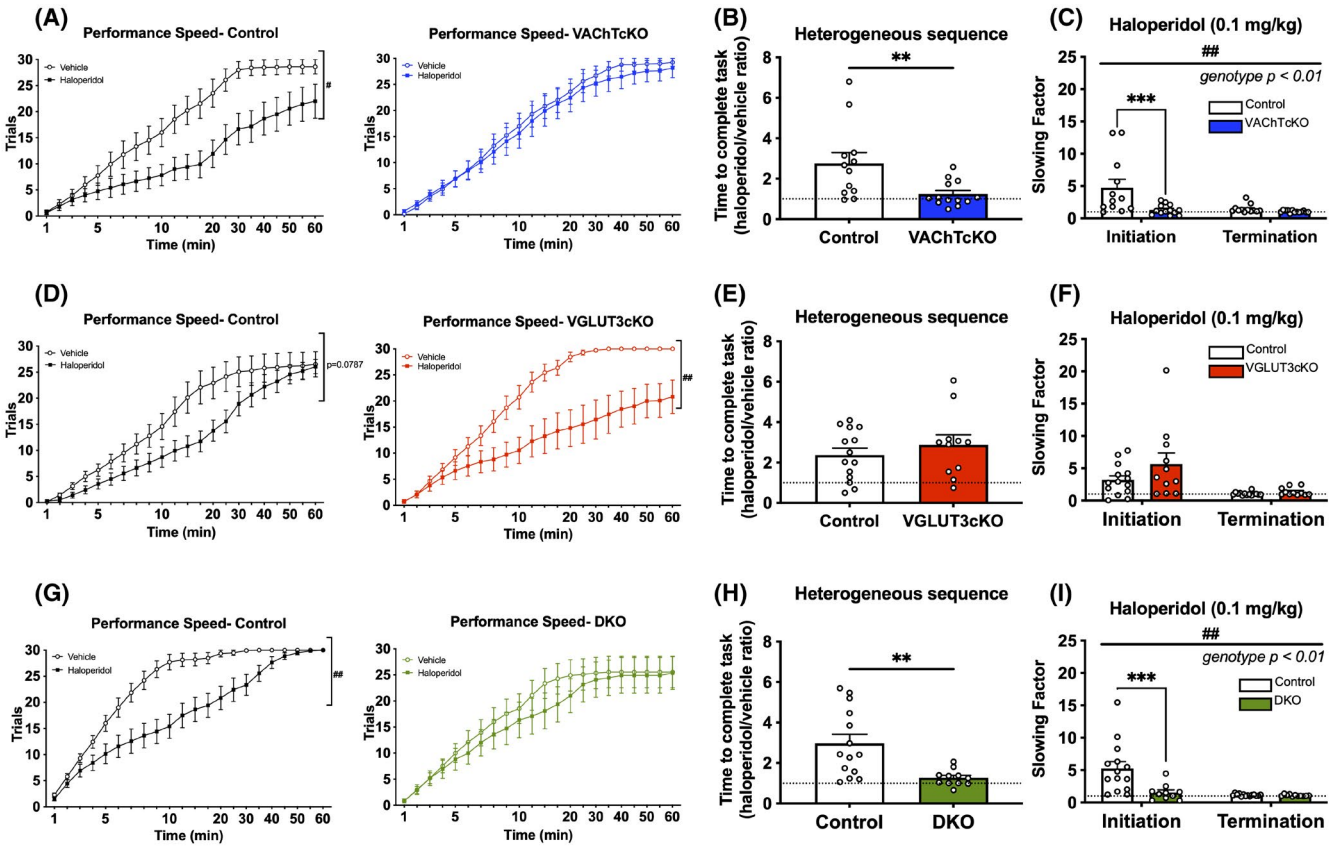

FIGURE 6 Haloperidol does not impair the touchscreen performance of mice with a loss of VAChT. (A–I) Parameters recorded during the heterogenous sequence touchscreen task when mice were treated with haloperidol (0.1 mg/kg) and vehicle: (A, D, G) performance speed over the course of the session, (B, E, H) time to complete 30 trials as a ratio of haloperidol to vehicle performance and (C, F, I) slowing factor during the initial and final steps of the sequence (speed at which task was started versus ended as a ratio of haloperidol latency versus saline latency). Data are expressed as mean ± SEM, *comparing to matched littermate control parameter, $^{\#}$overall genotype effect, $^{*}p < .05$, $^{**}p < .01$, $^{***}p < .001$. Summary statistics in Table S2

as terminal components were relatively unimpaired. Taken together, we find that when treated with haloperidol, VAChTcKO and VGLUT3cKO mice had differing, often opposite, responses to the drug. While mice lacking VAChT were unaffected by haloperidol's slowing down effect, mice lacking VGLUT3 were significantly slowed down, especially on early sequence components.

Notably, we found that the performance of DKO mice was almost unaltered by haloperidol. The performance speed (Figure 6G), overall time to complete the sequence task (Figure 6H) and number of blank touches (Figure S6G,H) did not differ when the mice were treated with haloperidol in comparison to vehicle. However, DKO mice showed a small increase in correct response latency across the grids 1–3, which was significantly less than that of littermate controls and showed a more pronounced increase in correct response latency on grids 4 and 5 (Figure S6I; Two-way ANOVA; main effect of genotype: $F(1,110) = 9.219$, $p = .0030$). Moreover, the performance of DKO mice in early and late sequence components was relatively unaffected (Figure 6I). Overall, the response of haloperidol administration in DKO mice was similar to what was observed with VAChTcKO mice and differed from VGLUT3cKO mice.

4 | DISCUSSION

In this study, we compared the functional consequences of the deletion of VAChT, VGLUT3 or both transporters in CINs. We show that interference with ACh or Glu have dissociable effects on dopamine dynamics regulated by a reward, sensitivity to the D2 antagonist haloperidol, and complex responses to sequential events (Summarized in Figure 7). Additionally, we found that deletion of both VAChT and VGLUT3 from CINs largely recapitulates the effect of VAChT deletion from CINs, albeit the phenotype is more severe. This finding suggests that ACh signalling in striatal microcircuits is the predominant driver of these reward-based behaviors.

We found that in the nucleus accumbens shell of freely behaving mice, interference with VAChT expression from CINs appears to negatively modulate dopamine signalling evoked by a behavioral stimulus, such as reward. In contrast, interference with VGLUT3 appears to prolong dopamine signalling. This dissociation of the effects of ACh and Glu on reward-evoked dopamine signalling is in agreement with recently published work that examines dopamine efflux in the nucleus accumbens in response to chemical stimulation.[13,50] Specifically, dopamine efflux induced by KCl in anesthetized mice with a deletion of VAChT or VGLUT3 from CINs was decreased or increased, respectively. These changes in dopamine synaptic transmission may be attributed to ACh and Glu affecting panels of presynaptic receptors (nAChR, mAChR, mGluRs) and/or dopamine clearance from the synapse.

In the striatum, it has been proposed that dopaminergic signalling drives sequential learning[55,56] with features of the dopamine signal, including its amplitude and duration, modulating the efficiency of reward-based learning in an operant task.[57–60] Since altering CIN neurotransmitter secretion changed dopamine signalling, we evaluated if operant behavior was also altered. Notably, we found that deletion of VAChT and VGLUT3 had contrasting

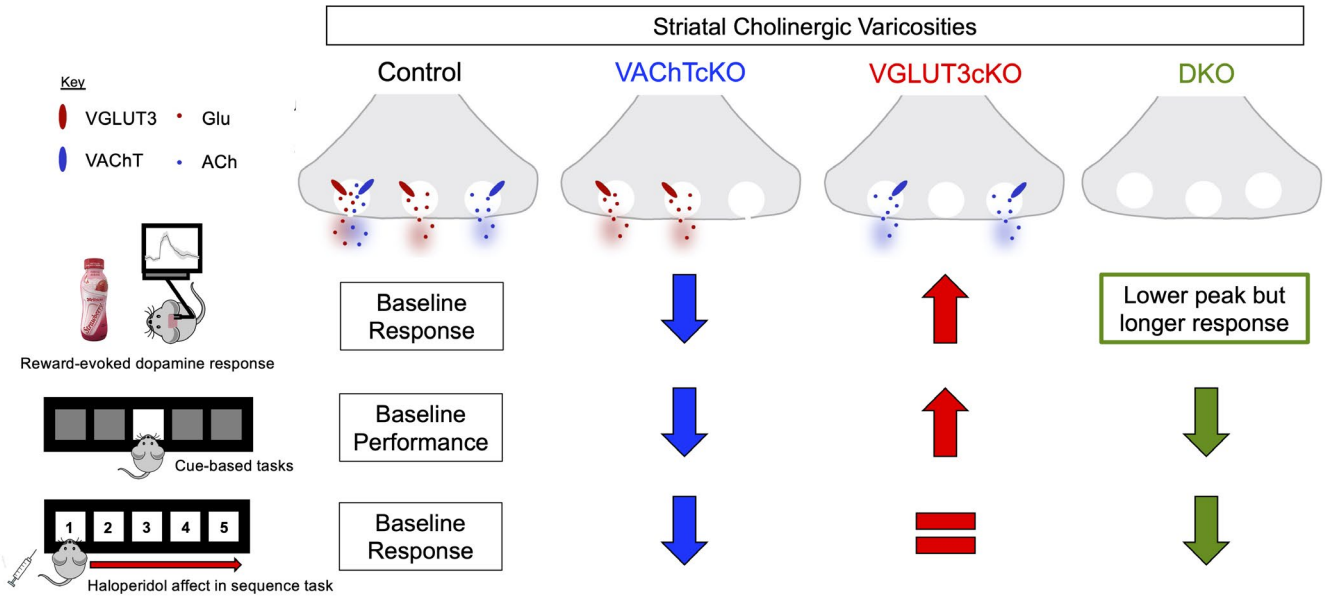

FIGURE 7 Summary of experimental findings

effects on performance in sequential response tasks. Loss of CIN-released ACh led to some difficulties in following a sequence of instrumental cues (illuminated grid positions) over 11 task sessions. Specifically, VAChTcKO mice seem to take longer to complete the heterogenous sequence task, especially during early learning and they had more difficulties identifying the cues as evidenced by an increased amount of blank touches. This was not associated with changes in locomotor behavior in a novel environment or impulsivity, as we have previously established that VAChTcKO mice behave similar to littermate controls in the locomotor box and 5-choice serial reaction time tasks.[13] In contrast, we found that loss of Glu release from CINs improved performance in cue-based tasks. Compared to controls, VGLUT3cKO mice were faster to learn the FR task and were quicker at completing early sessions of the heterogenous sequence task. Notably, VGLUT3cKO mice started the heterogenous sequence task at a quicker rate after several training days (faster initiation), suggesting better recognition of cues distal to the reward.[30] While VGLUT3cKO mice were hyperactive in a novel environment, this was not reflected in the latencies to complete stages of the touchscreen tasks. Whether these behavioral changes are directly related to altered dopamine signalling remains unclear and could be tested in the future by direct manipulations of dopamine secretion. To note, the bulk dopamine response recorded in our study may not reflect the millisecond by millisecond measures associated with behavior and consequently, recording dopamine dynamics during the actual touchscreen tasks would be most informative. Nonetheless, the observed opposing effect on operant behaviors in our study is in line with recently published work on behavioral flexibility.[13] Specifically, we previously found that mice with a loss of striatal VAChT are more prone to habits whereas mice with a loss of striatal VGLUT3 favor goal-directed behavior.[13]

It should also be noted that both ACh and Glu directly affect striatal function by mechanisms that are independent of dopamine, such as modulation of D1 and D2 medium spiny neurons (MSNs) directly[26,61,62] and indirectly, via the regulation of GABAergic interneurons.[63,64] To note, sequential responding has previously been associated with the activity of striatal MSNs, with these neurons signalling the initiation and termination of a specific action sequence.[56,65,66] Furthermore, Keeler et al. (2014) found that pharmacologically activating or inhibiting D2 signalling in wildtype rats impaired their ability to complete a heterogenous sequence task. This suggests that the D2 MSN pathway may drive response selection.[30] Since VAChTcKO mice had a slowed overall performance in the operant heterogenous sequence task (mimicking controls treated with haloperidol), it is possible that these mice have an altered D2 MSN pathway. In line with this idea, we found that treatment with the D2 antagonist, haloperidol did not change the touchscreen performance of VAChTcKO mice. In contrast, a loss of VGLUT3 from CINs changed how haloperidol affected touchscreen performance. Specifically, VGLUT3cKO mice took 3 times as long to complete the task. The reason for this distinction in drug effect is likely that the VAChTcKO mice are as impaired in their D2 MSN pathway as they can be, and further blocking D2 receptors has little effect. Nonetheless, it is possible that the effects reported herein are being partially mediated by D2 receptors on CINs themselves, instead of MSNs.[67] By modulating CIN-mediated signalling we could be interfering with their constitutive integrated stress response, a biochemical process that influences which proteins are synthesized in cholinergic striatal neurons.[68] In particular, this integrated stress response is required for normal D2R-modulation of CINs and changes in its functionality can affect the vigor of learned tasks.[68]

To evaluate if ACh and/or Glu are driving the observed behavioral changes, we also investigated reward-evoked dopamine release and reward-based learning in mice where CINs are incapable of releasing both neurotransmitters effectively (DKO mice). When examining dopamine signalling in the DKO mice, similar to VAChTcKO mice, DKO mice have a lower dopamine peak in the nucleus accumbens shell. However, the overall dopamine release of DKO mice is unchanged (area under the curve), owing to a prolonged response which mimics VGLUT3cKO mice. This finding suggests that ACh and Glu released by CIN seem to have additive and independent effects.

In contrast to the single KO mice (VAChTcKO, VGLUT3cKO), we found that DKO mice had more pronounced changes in performance in homogenous tasks (FR/PR). Specifically, DKO mice were slower to learn the initial tasks (FR1 task) but once they learned, they were more willing to work compared to controls (PR4 and PR8). However, this increased PR performance only manifested after two training days in the task. These mutant mice were also significantly impaired in the heterogenous sequence task. In particular, the DKO mice showed an increased level of responding, commonly on blank windows (often the central window), leading to them to take twice as long to complete the task when compared to their littermate controls. Together the changed performance in the operant tasks may suggest that DKO mice have aberrant habitual behavior. This is consistent with studies that show that ablation of CINs leads to deficits in behavioral flexibility and increased compulsive behavior.[69,70] Furthermore, this result is in line with our previous study that indicates altering neurotransmitter release from CINs disrupts the balance between goal directed and habitual behavior.[13] However, to confirm that DKO mice are indeed habitual future studies would require a devaluation paradigm to

be performed. Additionally, we have to consider that the enhanced nose-poking behavior could be impacted by locomotion as DKO mice are hyperactive in a novel environment. Nonetheless, we see minimal changes in correct and reward response latencies in the operant tasks. Furthermore, previous studies have shown that extensive training in touchscreen tasks can diminish hyperactivity if mice have intact habituation.[36]

Beyond the homogenous tasks, we consistently found that the behavior of DKO mice is similar to VAChTcKO mice: impaired in the heterogeneous sequence task and unresponsive to haloperidol's slowing down affect. This would suggest that ACh might be the predominant signalling molecule for driving the operant behavioral responses studied here. However, it is likely that this relationship is more complex and depends on the type of task and individual motivation to perform a task. Furthermore, it is likely that direct and indirect responses to ACh and Glu released by CINs on striatal MSNs collaborate with dopamine signalling to shape behavior. Interestingly, the overall behavioral changes in DKO mice do not reflect the additive influence of VAChT and VGLUT3 in dopamine release. Specifically, the dopamine release effects of VAChT and VGLUT3 single deletions seem to be combined in DKO mice where both lower amplitude and prolonged dopamine response is apparent, yet their behavior primarily reflects the VAChT deletion. This may suggest that changes in dopamine signaling are not simply translated into behavior and other parameters (changes in ACh and Glu release itself, compensational circuit alterations) are contributing to the final behavioral phenotype.

Our study primarily focuses on the basal ganglia as the striatum has been shown to regulate reward-based learning.[71,72] However, we have previously shown that the D2-Cre driver leads to a 50% decrease of VAChT levels in the cortex[13] which could also contribute to the behavioral phenotype observed in VAChTcKO and DKO mice. Nonetheless, the phenotypes of VAChTcKO mice are relatively mild in this study, indicating that the cortical VAChT decrease itself does not induce major changes in the studied behavior. Only when VGLUT3 was also deleted (DKO mice), presumably disrupting the function of striatal CINs, mice responded more in the PR task and were significantly more impaired in the heterogeneous sequence task. To separate the effect of striatal and cortical VAChT, in future studies it would be ideal to target the deletion of VAChT in the striatum of adult mice using viral vectors. Notably, we have previously shown that virally targeting VAChT in the DMS can recapitulate the impairments of goal-directed learning evident in VAChTcKO mice.[13] This viral approach would also rule out the involvement of developmental compensatory mechanisms on the endophenotypes herein uncovered. As mutant mice are born with decreased cholinergic and/or glutamatergic tone in the striatum, it is possible that compensatory changes may have occurred since birth and behavioral effects of ACh or Glu release are masked/modified. Nonetheless, even if a portion of the phenotype can be associated with developmental changes, this study still speaks to the distinct roles and contributions that two neurotransmitters have in striatal-dependent behaviors.

In conclusion, the data provide novel information into how the striatal network is regulated during behavior and clarify the differential impact of CIN-released ACh and Glu. It highlights the complexity that co-transmission brings to neuronal signaling and functional regulation. We found that ACh and Glu have opposing effects on operant responding which could be associated with changes in dopamine signaling and/or D2 pathways. Notably, we found that ACh release from CINs may drive the majority of behavioral responses, whereas Glu release seems to be mainly involved in refining behavioral outputs. Dual neurotransmitter neurons are found in multiple organisms, including flies, where they can regulate complex behaviors.[73] VGLUTs have been suggested to facilitate the loading of vesicles with ACh and other neuromodulators,[25,74–76] albeit VGLUTs and other neurotransmitter transporters may be segregated in different vesicles.[77] Our results illustrate potential reasons by which dual-transmitter neuronal systems could be favoured during evolution, beyond facilitating the release of one of the neurotransmitters. Neurons that release two neurotransmitters are poised to regulate a much wider repertoire of behavioral outcomes, likely by activating a more diverse set of receptors. Ultimately, understanding how dual transmitter systems are modulated in individual neurons and contribute to control behavior will help to decode how neuronal communication impacts neuronal representation of more sophisticated behavior repertoires.

ACKNOWLEDGMENTS

The authors thank Iris Villalobos Pineda, Sanda Raulic, Clara Man Ching Yau and Matthew Cowan for animal care and technical support. The authors also thank Jue Fan for support and for the generation of qPCR data for VAChT and VGLUT3 in tissue from double knockout mice. OK received an Ontario Graduate Student (OGS) Doctoral Award and the Jonathan and Joshua Graduate Scholarship. This research was supported by funds from Brain Canada Multi-Investigator Research Initiative (SEM, VFP, and MAMP), MAMP, VFP, LMS, and TJB contributions to this work received support from the Canadian Institutes of Health Research (CIHR, MOP 126000, MOP 136930, MOP 89919, PJT 162431, PJT 159781), Natural Science and Engineering Research Council of Canada (402524-2013 RGPIN; 03592-2021 RGPIN), Weston Brain

Institute (for development of touchscreen experiments) and a BrainsCAN/Canada First Research Excellence Fund Accelerator award as well as support for the Rodent Cognitive and Innovation Core. MAMP is a Tier I Canada Research Chair in Neurochemistry of Dementia. LSM is a Tier I Canada Research Chair in Translation Cognitive Neuroscience and a CIFAR Fellow in the Brain, Mind and Consciousness program. TJB is a Western Research Chair.

DISCLOSURES

TJB and LMS have established a series of targeted cognitive tests for animals, administered via touchscreen within a custom environment known as the "Bussey-Saksida touchscreen chamber." Cambridge Enterprise, the technology transfer office of the University of Cambridge, supported commercialization of the Bussey-Saksida chamber, culminating in a license to Campden Instruments. Any financial compensation received from commercialization of the technology is fully invested in further touchscreen development and/or maintenance.

AUTHOR CONTRIBUTIONS

Ornela Kljakic and Helena Janíčková designed and performed research, analyzed data, and wrote the paper. Miguel Skirzewski designed and performed research and analyzed data. Amy Reichelt performed research and Sara Memar, Salah El Mestikawy, Yulong Li and Lisa M. Saksida contributed new reagents or analytic tools. Timothy J. Bussey contributed new reagents or analytic tools and wrote the paper. Vania F. Prado and Marco A. M. Prado designed research, contributed new reagents or analytic tools, and wrote the paper. All authors were involved in revising the manuscript for intellectual content. All authors read and approved the final version of the manuscript.

DATA AVAILABILITY STATEMENT

The data that support the findings of this study are available in MouseBytes (www.mousebytes.ca). All the behavioral and molecular data for the figures can be found in the following repository: https://mousebytes.ca/compedit?repolinkguid=e46739ed-1154-4d85-bf8c-5cba6b677a74. Each mouse line has a subexperiment with one Excel analysis file provided for each touchscreen behavioral experiment. Each Excel file provides the raw data as well as the calculated parameters. Furthermore, the code used for analysis of the photometry data is also found in this repository.

The touchscreen raw data can also be downloaded directly from the Data Lab in mousebytes.ca, where other non-investigated parameters can also be extracted and examined. There are 6 associated experimental datasets.

REFERENCES

1. Guzman MS, De Jaeger X, Raulic S, et al. Elimination of the vesicular acetylcholine transporter in the striatum reveals regulation of behaviour by cholinergic-glutamatergic co-transmission. *PLoS Biol*. 2011;9(11):e1001194. doi:10.1371/journal.pbio.1001194
2. Kljakic O, Janickova H, Prado VF, Prado MAM. Cholinergic/glutamatergic co-transmission in striatal cholinergic interneurons: new mechanisms regulating striatal computation. *J Neurochem*. 2017;142:90-102. doi:10.1111/jnc.14003
3. Gerfen CR. Synaptic organization of the striatum. *J Electron Microsc Tech*. 1988;10(3):265-281. doi:10.1002/jemt.1060100305
4. Pisani A, Bernardi G, Ding J, Surmeier DJ. Re-emergence of striatal cholinergic interneurons in movement disorders. *Trends Neurosci*. 2007;30(10):545-553. doi:10.1016/j.tins.2007.07.008
5. Zhai S, Tanimura A, Graves SM, Shen W, Surmeier DJ. Striatal synapses, circuits, and Parkinson's disease. *Curr Opin Neurobiol*. 2018;48:9-16. doi:10.1016/j.conb.2017.08.004
6. Vonsattel JPG, DiFiglia M. Huntington disease. *J Neuropathol Exp Neurol*. 1998;57(5):369-384. doi:10.1097/00005072-199805000-00001
7. Lebouc M, Richard Q, Garret M, Baufreton J. Striatal circuit development and its alterations in Huntington's disease. *Neurobiol Dis*. 2020;145:105076. doi:10.1016/j.nbd.2020.105076
8. Koob GF. Neural mechanisms of drug reinforcement. *Ann N Y Acad Sci*. 1992;654:171-191.
9. Lobo MK, Nestler EJ. The striatal balancing act in drug addiction: distinct roles of direct and indirect pathway medium spiny neurons. *Front Neuroanat*. 2011;5:1-11. doi:10.3389/fnana.2011.00041
10. Saxena S, Brody AL, Schwartz JM, Baxter LR. Neuroimaging and frontal-subcortical circuitry in obsessive-compulsive disorder. *Br J Psychiatry*. 1998;173(S35):26-37. doi:10.1192/s0007125000297870
11. Pujol J, Soriano-Mas C, Alonso P, et al. Mapping structural brain alterations in obsessive-compulsive disorder. *Arch Gen Psychiatry*. 2004;61(7):720. doi:10.1001/archpsyc.61.7.720
12. Fladung A-K, Grön G, Grammer K, et al. A neural signature of anorexia nervosa in the ventral striatal reward system. *Am J Psychiatry*. 2010;167(2):206-212. doi:10.1176/appi.ajp.2009.09010071
13. Favier M, Janickova H, Justo D, et al. Cholinergic dysfunction in the dorsal striatum promotes habit formation and maladaptive eating. *J Clin Invest*. 2020;130(12):6616-6630. doi:10.1172/JCI138532
14. Brunelin J, Fecteau S, Suaud-Chagny M-F. Abnormal striatal dopamine transmission in schizophrenia. *Curr Med Chem*. 2013;20(3):397-404. doi:10.2174/0929867311320030011
15. Kegeles LS, Abi-Dargham A, Frankle WG, et al. Increased synaptic dopamine function in associative regions of the striatum in schizophrenia. *Arch Gen Psychiatry*. 2010;67(3):231. doi:10.1001/archgenpsychiatry.2010.10
16. Aylward EH, Roberts-Twillie JV, Barta PE, et al. Basal ganglia volumes and white matter hyperintensities in patients with bipolar disorder. *Am J Psychiatry*. 1994;151(5):687-693. doi:10.1176/ajp.151.5.687
17. Karcher NR, Rogers BP, Woodward ND. Functional connectivity of the striatum in schizophrenia and psychotic bipolar disorder.

Biol Psychiatry Cogn Neurosci Neuroimaging. 2019;4(11):956-965. doi:10.1016/j.bpsc.2019.05.017

18. Dautan D, Huerta-Ocampo I, Witten IB, et al. A major external source of cholinergic innervation of the striatum and nucleus accumbens originates in the brainstem. *J Neurosci*. 2014;34(13):4509-5418. doi:10.1523/JNEUROSCI.5071-13.2014
19. Abudukeyoumu N, Hernandez-Flores T, Garcia-Munoz M, Arbuthnott GW. Cholinergic modulation of striatal microcircuits. *Eur J Neurosci*. 2019;49(5):604-622. doi:10.1111/ejn.13949
20. Gonzales KK, Smith Y. Cholinergic interneurons in the dorsal and ventral striatum: anatomical and functional considerations in normal and diseased conditions. *Ann N Y Acad Sci*. 2015;1349(1):1-45. doi:10.1111/nyas.12762
21. Lim SAO, Kang UJ, McGehee DS. Striatal cholinergic interneuron regulation and circuit effects. *Front Synaptic Neurosci*. 2014;6:1-23. doi:10.3389/fnsyn.2014.00022
22. Prado VF, Janickova H, Al-Onaizi MA, Prado MAM. Cholinergic circuits in cognitive flexibility. *Neuroscience*. 2017;345:130-141. doi:10.1016/j.neuroscience.2016.09.013
23. Cachope R, Mateo Y, Mathur B, et al. Selective activation of cholinergic interneurons enhances accumbal phasic dopamine release: setting the tone for reward processing. *Cell Rep*. 2012;2(1):33-41. doi:10.1016/j.celrep.2012.05.011
24. Threlfell S, Lalic T, Platt NJ, Jennings KA, Deisseroth K, Cragg SJ. Striatal dopamine release is triggered by synchronized activity in cholinergic interneurons. *Neuron*. 2012;75(1):58-64. doi:10.1016/j.neuron.2012.04.038
25. Gras C, Amilhon B, Lepicard ÈM, et al. The vesicular glutamate transporter VGLUT3 synergizes striatal acetylcholine tone. *Nat Neurosci*. 2008;11(3):292-300. doi:10.1038/nn2052
26. Higley MJ, Gittis AH, Oldenburg IA, et al. Cholinergic interneurons mediate fast VGluT3-dependent glutamatergic transmission in the striatum. *PLoS One*. 2011;6(4):e19155. doi:10.1371/journal.pone.0019155
27. Nelson AB, Bussert TG, Kreitzer AC, Seal RP. Striatal cholinergic neurotransmission requires VGLUT3. *J Neurosci*. 2014;34(26):8772-8777. doi:10.1523/JNEUROSCI.0901-14.2014
28. Gangarossa G, Guzman M, Prado VF, et al. Role of the atypical vesicular glutamate transporter VGLUT3 in l-DOPA-induced dyskinesia. *Neurobiol Dis*. 2016;87:69-79. doi:10.1016/j.nbd.2015.12.010
29. Guzman MS, De Jaeger X, Drangova M, Prado MAM, Gros R, Prado VF. Mice with selective elimination of striatal acetylcholine release are lean, show altered energy homeostasis and changed sleep/wake cycle. *J Neurochem*. 2013;124(5):658-669. doi:10.1111/jnc.12128
30. Keeler JF, Pretsell DO, Robbins TW. Functional implications of dopamine D1 vs. D2 receptors: a "prepare and select" model of the striatal direct vs. indirect pathways. *Neuroscience*. 2014;282:156-175. doi:10.1016/j.neuroscience.2014.07.021
31. Martins-Silva C, De Jaeger X, Guzman MS, et al. Novel strains of mice deficient for the vesicular acetylcholine transporter: insights on transcriptional regulation and control of locomotor behavior. *PLoS One*. 2011;6(3):e17611. doi:10.1371/journal.pone.0017611
32. Fasano C, Rocchetti J, Pietrajtis K, et al. Regulation of the hippocampal network by VGLUT3-positive CCK- GABAergic basket cells. *Front Cell Neurosci*. 2017;11(140):1-15. doi:10.3389/fncel.2017.00140
33. Divito CB, Steece-Collier K, Case DT, et al. Loss of VGLUT3 produces circadian-dependent hyperdopaminergia and ameliorates motor dysfunction and L-dopa-mediated dyskinesias in a model of Parkinson's disease. *J Neurosci*. 2015;35(45):14983-14999. doi:10.1523/jneurosci.2124-15.2015
34. Gong S, Doughty M, Harbaugh CR, et al. Targeting Cre recombinase to specific neuron populations with bacterial artificial chromosome constructs. *J Neurosci*. 2007;27(37):9817-9823. doi:10.1523/JNEUROSCI.2707-07.2007
35. Kolisnyk B, Al-Onaizi MA, Prado VF, Prado MAM. α7 Nicotinic ACh receptor-deficient mice exhibit sustained attention impairments that are reversed by β2 nicotinic ACh receptor activation. *Br J Pharmacol*. 2015;172(20):4919-4931. doi:10.1111/bph.13260
36. Kolisnyk B, Al-Onaizi MA, Hirata PHF, et al. Forebrain deletion of the vesicular acetylcholine transporter results in deficits in executive function, metabolic, and RNA splicing abnormalities in the prefrontal cortex. *J Neurosci*. 2013;33(37):14908-14920. doi:10.1523/JNEUROSCI.1933-13.2013
37. Romberg C, Horner AE, Bussey TJ, Saksida LM. A touch screen-automated cognitive test battery reveals impaired attention, memory abnormalities, and increased response inhibition in the TgCRND8 mouse model of Alzheimer's disease. *Neurobiol Aging*. 2013;34(3):731-744. doi:10.1016/j.neurobiolaging.2012.08.006
38. Beraldo FH, Thomas A, Kolisnyk B, et al. Hyperactivity and attention deficits in mice with decreased levels of stress-inducible phosphoprotein 1 (STIP1). *DMM Dis Model Mech*. 2015;8(11):1457-1466. doi:10.1242/dmm.022525
39. Kilkenny C, Browne WJ, Cuthill IC, Emerson M, Altman DG. Improving bioscience research reporting: the arrive guidelines for reporting animal research. *Animals*. 2014;4(1):35-44. doi:10.3390/ani4010035
40. Sun F, Zhou J, Dai B, et al. Next-generation GRAB sensors for monitoring dopaminergic activity in vivo. *Nat Methods*. 2020;17(11):1156-1166. doi:10.1038/s41592-020-00981-9
41. Paxinos G, Franklin KBJ. *The Mouse Brain in Stereotaxic Coordinates*. 2nd ed. Academic Press; 2001.
42. Al-Onaizi MA, Parfitt GM, Kolisnyk B, et al. Regulation of cognitive processing by hippocampal cholinergic tone. *Cereb Cortex*. 2017;27(2):1615-1628. doi:10.1093/cercor/bhv349
43. Kolisnyk B, Al-Onaizi MA, Hirata PHF, et al. Forebrain deletion of the vesicular acetylcholine transporter results in deficits in executive function, metabolic, and RNA splicing abnormalities in the prefrontal cortex. *J Neurosci*. 2013;33(37):14908-14920. doi:10.1523/JNEUROSCI.1933-13.2013
44. Kolisnyk B, Guzman MS, Raulic S, et al. ChAT-ChR2-EYFP mice have enhanced motor endurance but show deficits in attention and several additional cognitive domains. *J Neurosci*. 2013;33(25):10427-10438. doi:10.1523/JNEUROSCI.0395-13.2013
45. Heath CJ, Phillips BU, Bussey TJ, Saksida LM. Measuring motivation and reward-related decision making in the rodent operant touchscreen system. *Curr Protoc Neurosci*. 2016;74:8.34.1-8.34.20. doi:10.1002/0471142301.ns0834s74
46. Nithianantharajah J, Grant SGN. Cognitive components in mice and humans: combining genetics and touchscreens for medical translation. *Neurobiol Learn Mem*. 2013;105:13-19. doi:10.1016/j.nlm.2013.06.006
47. Janickova H, Kljakic O, Robbins TW, et al. Evaluating sequential response learning in the rodent operant touchscreen system. *Curr Protoc*. 2021;1(10):e268. doi:10.1002/CPZ1.268
48. Prado VF, Martins-Silva C, de Castro BM, et al. Mice deficient for the vesicular acetylcholine transporter are myasthenic and have deficits in object and social recognition. *Neuron*. 2006;51(5):601-612. doi:10.1016/j.neuron.2006.08.005

49. Joviano-Santos JV, Kljakic O, Magalhães-Gomes MPS, et al. Motoneuron-specific loss of VAChT mimics neuromuscular defects seen in congenital myasthenic syndrome. *FEBS J*. 2021;288(18):5331-5349. doi:10.1111/FEBS.15825
50. Sakae DY, Marti F, Lecca S, et al. The absence of VGLUT3 predisposes to cocaine abuse by increasing dopamine and glutamate signaling in the nucleus accumbens. *Mol Psychiatry*. 2015;20(11):1148-1159. doi:10.1038/mp.2015.104
51. Schultz W, Dayan P, Montague PR. A neural substrate of prediction and reward. *Science*. 1997;275(5306):1593-1599. doi:10.1126/science.275.5306.1593
52. Schultz W. Predictive reward signal of dopamine neurons. *J Neurophysiol*. 1998;80(1):1-27. doi:10.1152/jn.1998.80.1.1
53. Palmer D, Creighton S, Prado VF, Prado MAM, Choleris E, Winters BD. Mice deficient for striatal Vesicular Acetylcholine Transporter (VAChT) display impaired short-term but normal long-term object recognition memory. *Behav Brain Res*. 2016;311:267-278. doi:10.1016/j.bbr.2016.05.050
54. Salamone JD, Cousins MS, Bucher S. Anhedonia or anergia? Effects of haloperidol and nucleus accumbens dopamine depletion on instrumental response selection in a T-maze cost/benefit procedure. *Behav Brain Res*. 1994;65(2):221-229. doi:10.1016/0166-4328(94)90108-2
55. Wassum KM, Ostlund SB, Maidment NT. Phasic mesolimbic dopamine signaling precedes and predicts performance of a self-initiated action sequence task. *Biol Psychiatry*. 2012;71(10):846-854. doi:10.1016/j.biopsych.2011.12.019
56. Jin X, Costa RM. Start/stop signals emerge in nigrostriatal circuits during sequence learning. *Nature*. 2010;466(7305):457-462. doi:10.1038/nature09263
57. Kim KM, Baratta MV, Yang A, Lee D, Boyden ES, Fiorillo CD. Optogenetic mimicry of the transient activation of dopamine neurons by natural reward is sufficient for operant reinforcement. *PLoS One*. 2012;7(4):e33612. doi:10.1371/journal.pone.0033612
58. Tsai H-C, Zhang F, Adamantidis A, et al. Phasic firing in dopaminergic neurons is sufficient for behavioral conditioning. *Science*. 2009;324(5930):1080-1084. doi:10.1126/science.1168878
59. Schultz W, Apicella P, Ljungberg T. Responses of monkey dopamine neurons to reward and conditioned stimuli during successive steps of learning a delayed response task. *J Neurosci*. 1993;13(3):900-913. doi:10.1523/jneurosci.13-03-00900.1993
60. Smith-Roe SL, Kelley AE. Coincident activation of NMDA and dopamine D1 receptors within the nucleus accumbens core is required for appetitive instrumental learning. *J Neurosci*. 2000;20(20):7737-7742. doi:10.1523/jneurosci.20-20-07737.2000
61. Bernard V, Normand E, Bloch B. Phenotypical characterization of the rat striatal neurons expressing muscarinic receptor genes. *J Neurosci*. 1992;12(9):3591-3600. doi:10.1523/jneurosci.12-09-03591.1992
62. Yan Z, Flores-Hernandez J, Surmeier DJ. Coordinated expression of muscarinic receptor messenger RNAs in striatal medium spiny neurons. *Neuroscience*. 2001;103(4):1017-1024. doi:10.1016/S0306-4522(01)00039-2
63. De Rover M, Lodder JC, Kits KS, Schoffelmeer ANM, Brussaard AB. Cholinergic modulation of nucleus accumbens medium spiny neurons. *Eur J Neurosci*. 2002;16(12):2279-2290. doi:10.1046/j.1460-9568.2002.02289.x
64. Sullivan MA, Chen H, Morikawa H. Recurrent inhibitory network among striatal cholinergic interneurons. *J Neurosci*. 2008;28(35):8682-8690. doi:10.1523/JNEUROSCI.2411-08.2008
65. Jin X, Tecuapetla F, Costa RM. Basal ganglia subcircuits distinctively encode the parsing and concatenation of action sequences. *Nat Neurosci*. 2014;17(3):423-430. doi:10.1038/nn.3632
66. Tecuapetla F, Jin X, Lima SQ, Costa RM. Complementary contributions of striatal projection pathways to action initiation and execution. *Cell*. 2016;166(3):703-715. doi:10.1016/j.cell.2016.06.032
67. Kharkwal G, Brami-Cherrier K, Lizardi-Ortiz José E, et al. Parkinsonism driven by antipsychotics originates from dopaminergic control of striatal cholinergic interneurons. *Neuron*. 2016;91(1):67-78. doi:10.1016/j.neuron.2016.06.014
68. Helseth AR, Hernandez-Martinez R, Hall VL, et al. Cholinergic neurons constitutively engage the ISR for dopamine modulation and skill learning in mice. *Science*. 2021;372(6540):eabe1931. doi:10.1126/science.abe1931
69. Aoki S, Liu AW, Zucca A, Zucca S, Wickens JR. Role of striatal cholinergic interneurons in set-shifting in the rat. *J Neurosci*. 2015;35(25):9424-9431. doi:10.1523/JNEUROSCI.0490-15.2015
70. Martos YV, Braz BY, Beccaria JP, Murer MG, Belforte JE. Compulsive social behavior emerges after selective ablation of striatal cholinergic interneurons. *J Neurosci*. 2017;37(11):2849-2858. doi:10.1523/JNEUROSCI.3460-16.2017
71. Redgrave P, Prescott TJ, Gurney K. The basal ganglia: a vertebrate solution to the selection problem? *Neuroscience*. 1999;89(4):1009-1023. doi:10.1016/S0306-4522(98)00319-4
72. Balleine BW, O'Doherty JP. Human and rodent homologies in action control: corticostriatal determinants of goal-directed and habitual action. *Neuropsychopharmacology*. 2010;35:48-69. doi:10.1038/npp.2009.131
73. Sherer LM, Catudio Garrett E, Morgan HR, et al. Octopamine neuron dependent aggression requires dVGLUT from dual-transmitting neurons. *PLoS Genet*. 2020;16(2):e1008609. doi:10.1371/journal.pgen.1008609
74. Aguilar JI, Dunn M, Mingote S, et al. Neuronal depolarization drives increased dopamine synaptic vesicle loading via VGLUT. *Neuron*. 2017;95(5):1074-1088.e7. doi:10.1016/j.neuron.2017.07.038
75. Trudeau LE, El Mestikawy S. Glutamate cotransmission in cholinergic, GABAergic and monoamine systems: contrasts and commonalities. *Front Neural Circuits*. 2018;12:1-11. doi:10.3389/fncir.2018.00113
76. El Mestikawy S, Wallén-Mackenzie Å, Fortin GM, Descarries L, Trudeau LE. From glutamate co-release to vesicular synergy: vesicular glutamate transporters. *Nat Rev Neurosci*. 2011;12(4):204-216. doi:10.1038/nrn2969
77. Silm K, Yang J, Marcott PF, et al. Synaptic vesicle recycling pathway determines neurotransmitter content and release properties. *Neuron*. 2019;102(4):786-800.e5. doi:10.1016/j.neuron.2019.03.031

SUPPORTING INFORMATION

Additional supporting information may be found in the online version of the article at the publisher's website.

How to cite this article: Kljakic O, Janíčková H, Skirzewski M, et al. Functional dissociation of behavioral effects from acetylcholine and glutamate released from cholinergic striatal interneurons. *FASEB J*. 2022;36:e22135. doi:10.1096/fj.202101425R